Metastatic phenotype and immunosuppressive tumour microenvironment in pancreatic ductal adenocarcinoma: Key role of the urokinase plasminogen activator (PLAU)

S. M. Zahid Hosen[1,2], Md. Nazim Uddin[3], Zhihong Xu[1,2], Benjamin J. Buckley[4,5], Chamini Perera[1,2], Tony C. Y. Pang[1,6], Alpha Raj Mekapogu[1,2], Mohammad Ali Moni[7], Faiyaz Notta[8], Steven Gallinger[8], Ron Pirola[1], Jeremy Wilson[1], Marie Ranson[4,5], David Goldstein[9,10] and Minoti Apte[1,2]*

[1]Pancreatic Research Group, SWS Clinical Campus, School of Clinical Medicine, Faculty of Medicine and Health, UNSW Sydney, Sydney, NSW, Australia, [2]Ingham Institute for Applied Medical Research, Liverpool, NSW, Australia, [3]Institute of Food Science and Technology, Bangladesh Council of Scientific and Industrial Research (BCSIR), Dhaka, Bangladesh, [4]Molecular Horizons and School of Chemistry & Molecular Bioscience, Faculty of Science, Medicine and Health, University of Wollongong, Wollongong, NSW, Australia, [5]Illawarra Health and Medical Research Institute, Wollongong, NSW, Australia, [6]Westmead Clinical School, Faculty of Medicine and Health, University of Sydney, The University of Sydney, Sydney, NSW, Australia, [7]School of Health and Rehabilitation Sciences, Faculty of Health and Behavioural Sciences, The University of Queensland, St Lucia, QLD, Australia, [8]PanCuRx Translational Research Initiative, Ontario Institute for Cancer Research, Toronto, ON, Canada, [9]Prince of Wales Clinical School, University of New South Wales, Sydney, NSW, Australia, [10]Department of Medical Oncology, Prince of Wales Hospital, Randwick, NSW, Australia

Background: Previous studies have revealed the role of dysregulated urokinase plasminogen activator (encoded by *PLAU*) expression and activity in several pathways associated with cancer progression. However, systematic investigation into the association of *PLAU* expression with factors that modulate PDAC (pancreatic ductal adenocarcinoma) progression is lacking, such as those affecting stromal (pancreatic stellate cell, PSC)-cancer cell interactions, tumour immunity, PDAC subtypes and clinical outcomes from potential *PLAU* inhibition.

Methods: This study used an integrated bioinformatics approach to identify prognostic markers correlated with PLAU expression using different transcriptomics, proteomics, and clinical data sets. We then determined the association of dysregulated *PLAU* and correlated signatures with oncogenic pathways, metastatic phenotypes, stroma, immunosuppressive tumour microenvironment (TME) and clinical outcome. Finally, using an *in vivo*

orthotopic model of pancreatic cancer, we confirmed the predicted effect of inhibiting PLAU on tumour growth and metastasis.

Results: Our analyses revealed that *PLAU* upregulation is not only associated with numerous other prognostic markers but also associated with the activation of various oncogenic signalling pathways, aggressive phenotypes relevant to PDAC growth and metastasis, such as proliferation, epithelial-mesenchymal transition (EMT), stemness, hypoxia, extracellular cell matrix (ECM) degradation, upregulation of stromal signatures, and immune suppression in the tumour microenvironment (TME). Moreover, the upregulation of *PLAU* was directly connected with signalling pathways known to mediate PSC-cancer cell interactions. Furthermore, *PLAU* upregulation was associated with the aggressive basal/squamous phenotype of PDAC and significantly reduced overall survival, indicating that this subset of patients may benefit from therapeutic interventions to inhibit *PLAU* activity. Our studies with a clinically relevant orthotopic pancreatic model showed that even short-term PLAU inhibition is sufficient to significantly halt tumour growth and, importantly, eliminate visible metastasis.

Conclusion: Elevated *PLAU* correlates with increased aggressive phenotypes, stromal score, and immune suppression in PDAC. *PLAU* upregulation is also closely associated with the basal subtype type of PDAC; patients with this subtype are at high risk of mortality from the disease and may benefit from therapeutic targeting of *PLAU*.

1 Introduction

Pancreatic ductal adenocarcinoma (PDAC), the most common subtype of pancreatic cancer (PC), is currently the seventh leading cause of cancer-associated death (1) and has a notoriously dismal prognosis. The incidence of PDAC continues to increase, and it is projected to become the second most common cause of cancer-linked death by 2030 (2). Current treatments have limited impact. The mean overall survival of the current standard treatment of FOLFIRINOX is 12.5 months, and that of Gemcitabine plus Abraxane, 10.3 months, P = 0.05 (3). Immunotherapies, individually or in combination with chemoradiotherapy or targeted therapy, have not made much progress in PDAC (4–7), reflecting an urgent need to identify new biologically driven targets to limit PDAC progression, particularly metastasis, the primary driver of mortality in this disease.

PDAC is no longer considered one disease at the molecular level, with many different molecular subtypes and subtype-specific treatment responses in PDAC (4–6). The two major transcriptomic-based subtypes, which have been confirmed across multiple investigations, are the classical/pancreatic progenitor subtype and the quasi-mesenchymal/basal-like/squamous subtype (4, 5, 8). The basal subtype is over-represented amongst metastatic PDAC tumours, and it is distinguished by ECM-rich activated stroma, the upregulation of expression of laminins and keratins and enriched for genes associated with epithelial-mesenchymal transition (EMT) and TGF-β signalling (9). On the other hand, the classical PDAC signature is characterised by upregulation of a wide range of transcription factors, GATA4, GATA6, NKX2-2 and HNF1A, associated with pancreatic lineage differentiation (4–8). Clinicopathologically, basal-type tumours are poorly differentiated and correlate with a worse prognosis (median OS 10–19.2 months and DFS 4.6–10.9); these tumours are chemoresistant but may have a better response to adjuvant therapy (4–6, 9–13). In contrast, classical type tumours are well-differentiated and are correlated with an overall better prognosis (median OS 19–43.1 months and DFS 13.5–20.6) (4, 6, 8, 10, 14–17).

Histologically, PDAC is well known to be characterised by a prominent stromal reaction comprising non-cellular elements like collagen, fibronectin, glycoproteins, proteoglycans, hyaluronic acid, cytokines, growth factors, and serine protein acidic and rich in cysteine (SPARC), as well as a wide range of cell types including neural, endothelial, immune & pancreatic stellate cells (PSCs). Pancreatic stellate cells (PSCs) are responsible for producing this excessive collagenous stroma in PDAC (18–20). Reciprocal interactions between activated pancreatic stellate and PDAC cells facilitate PDAC development and progression. One of the key pathways that may mediate cancer-stromal interactions is the hepatocyte growth factor (HGF) and its receptor c-MET pathway. Hyperactivity of HGF/c-MET signalling is considered a hallmark of cancer. Further, the serine protease urokinase plasminogen activator (uPA, encoded by *PLAU*) activates pro-HGF (secreted by pancreatic stellate cells) to active HGF, which binds to the c-MET receptor on cancer cells, activating several downstream signalling molecules. In addition, HGF binding to the c-MET receptor induces *PLAU* production by pancreatic and other cancer cells. The increased uPA level further activates pro-HGF, resulting in a feed-forward activation loop to promote cancer progression (21–23).

In normal cells (24–27), *PLAU* expression is very low and tightly controlled (7, 23, 28). However, *PLAU* and subsequently uPA expression is increased several-fold in tumour cells (23, 29–31), which results in catalytic conversion of inactive plasminogen to plasmin. Plasmin degrades extracellular matrix directly or indirectly *via* activation of precursor forms of matrix-degrading enzymes (matrix metalloproteinases) (32). Furthermore, in cancer cells, direct interaction of uPA with its receptor uPAR (encoded by PLAUR) facilitates the activation of multiple intracellular cell-signalling pathways, which regulate proliferation, migration, invasion, epithelial-mesenchymal transition, stem cell-like properties, release from states of dormancy, cell survival, chemoresistance, angiogenesis and vasculogenic mimicry (7, 24–27, 33–41) in cancer. All of which suggests a role as a master regulator in cancer development and progression. Indeed, upregulation of *PLAU* is associated with poor prognosis in several different cancers (33, 42). One study analysed 8 PDAC versus normal tissue gene expression profiles retrieved from the GEO database and found *PLAU* and *PLAU*R to be one of 10 hub genes significantly associated with PDAC pathogenesis (43).

This is the first study to delineate the role of the *PLAU* by integrated publically available transcriptomic, proteomics, and clinical data to 1) further elucidate the mechanisms underlying *PLAU*-related PDAC growth and progression, 2) use this data to undertake analyses of prognostic outcomes (overall survival) and assessment of relationship with clinical attributes, 3) identify the most 'at risk' group based on *PLAU* expression and4) preclinically assess selective uPA inhibition on pancreatic cancer growth and metastasis. To the best of our knowledge, this is the first integrated–omics analysis of the expression of these key components of the uPA system in PDAC.

2 Materials and methods

This study was implemented according to the analytical approach shown in Figure 1. The main steps involved in this task were step 1) identification of differentially expressed *PLAU* mRNA in i) 33 different cancer cohorts in the TCGA database, ii) different cancer cell lines from CCLE and iii) different GEO datasets. Step 2) Kaplan-Meier survival analyses of *PLAU* in PDAC-specific TCGA, ICGC and OICR patient cohorts. Step 3) Identifying other gene signatures correlated with *PLAU* from TCGA, ICGC and OICR patients cohorts. These gene signatures were mainly related to cancer cell functions, immunity and prognosis. A PPI network was constructed based on the gene signatures, and relevant subcellular pathways were identified. Step 4) Assessing the correlation of *PLAU* expression with pathways responsible for PSC-PDAC cell interactions. Step 5) Validation of transcriptome-based prognostic signatures using CPTAC proteomics data and assessing the relationship with clinical attributes. Step 6) Stratifying patient groups according to PLAU protein expression and survival and identifying the most 'at risk' group. Step 7) Further validation of the effect of PLAU inhibition on PDAC tumour growth and metastasis using *in vivo* pancreatic orthotopic model.

2.1 Datasets

We used the GEPIA (Gene Expression Profiling Interactive Analysis) TCGA dataset (http://gepia.cancer-pku.cn/) for comparing the differential mRNA expression of *PLAU* between cancer and normal samples. The Cancer Cell Line Encyclopedia (CCLE) (https://www.broadinstitute.org/ccle) mRNA expression data was used to identify distinctively upregulated *PLAU* in pancreatic cancer cell lines (44, 45). Next, we used different microarray data sets, including GSE16515 (46), GSE58561 (47), GSE71989 (48), GSE62165 (12), GSE71729 (6), and RNAseq GSE119794 (49) from the NCBI-GEO database.

Messenger RNA expression data and associated clinicopathological data were used from The Cancer Genome Atlas (TCGA, http://cancergenome.nih.gov/) and the International Cancer Genome Consortium (ICGC, https://icgc.org/). In particular, normalised gene expression of NGS was downloaded from the cBioPortal, (TCGA, Firehose https://www.cbioportal.org/) (50) on 1st July 2021. For the ICGC-Pancreatic Cancer - Australia (ICGC-PACA-AU) cohort, data were obtained from the Supplementary Material of the corresponding publication (4). In addition, we also used the Ontario Institute for Cancer Research (OICR) PDAC cohort (EGAS00001002543) for gene expression and clinical data through a data access
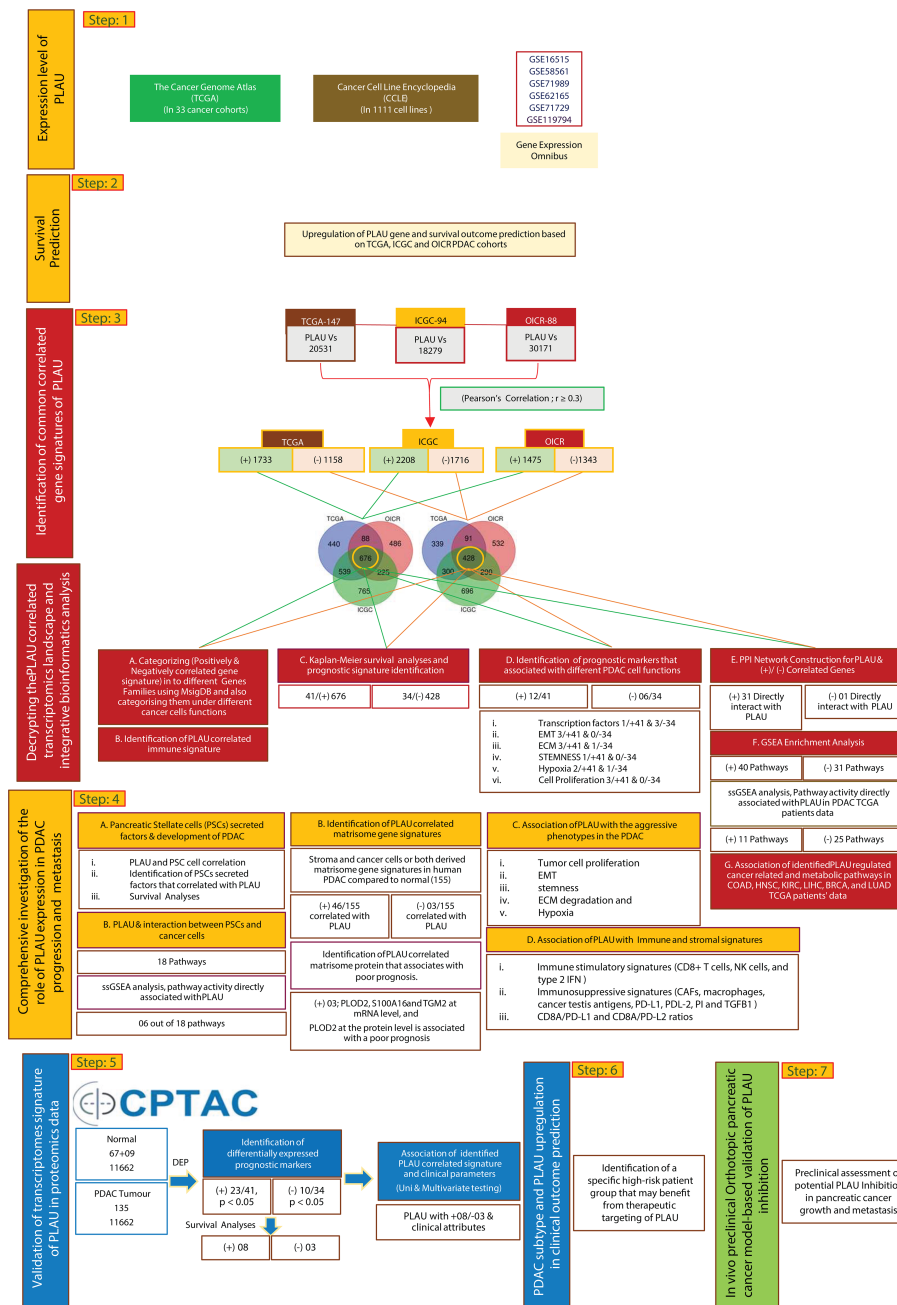
FIGURE 1

An integrative clinical bioinformatics workflow to decipher the role of *PLAU* in PDAC growth and progression, clinical outcome prediction and *in vivo* preclinical method-based validation of *PLAU* inhibition effects in tumour growth and metastasis.

agreement. Likewise, the proteomic and accompanying clinicopathological data from the proteogenomic characterisation of the PDAC study (6) was acquired *via* the Clinical Proteomic Tumor Analysis Consortium (CPTAC, https://cptac-data-portal.georgetown.edu/). Only PDAC cases with matched RNAseq/protein expression and clinical data were included in the analysis for all the cohorts.

2.2 Differential expression analysis

Differential expression analysis was performed using GEO2R (http://www.ncbi.nlm.nih.gov/geo/geo2r) and R packages limma from the Bioconductor project (http://www.bioconductor.org/). The thresholds of P-value < 0.05 and |FC| (fold change) > one was set to determine the significant level.

2.3 Identification of correlated gene signature

We used Pearson's correlation test to identify gene-gene correlation because the expression data is normally distributed. However, we employed Spearman's correlation test between the mRNA expression level of *PLAU* and the ssGSEA score of selected pathways because the data is not normally distributed. The threshold of our correlation analysis was set at greater than 0.30, and FDR ≤0.05. A false discovery rate (FDR) calculated by the Benjamini and Hochberg method (51) was used to adjust for multiple tests.

By comparing annotated gene sets from the Molecular Signatures Database (MSigDB) (52), and using the online tool "Calculate and draw custom Venn diagrams" (http://bioinformatics.psb.ugent.be/webtools/Venn/) we identified common tumour suppressors, oncogenes, translocated cancer genes, transcription factors, cytokines and growth factors, protein kinases, homeodomain proteins, and cell differentiation markers among positive and negatively correlated gene signatures of *PLAU* identified from three PDAC cohorts.

2.4 Gene-set enrichment analysis

We performed gene-set enrichment analysis of the *PLAU*-correlated genes using GSEA (53) with a false discovery rate threshold, FDR < 0.05. The Kyoto Encyclopedia of Genes and Genomes (KEGG) pathways that were significantly associated with the positive and the negatively *PLAU*-correlated genes were also identified (FDR < 0.05).

2.5 Functional analysis

We constructed protein-protein interaction (PPI) networks of the *PLAU*-correlated genes using the STRING (version v11 (54)) and visualised the PPI networks by utilising the Cytoscape 3.9.1 software (55). The rank of genes was identified by the Cytoscape plugin cytoHubba (56). Hub nodes were identified using a threshold of medium interaction score ≥0.40, and we selected the degree of interaction ≥25 for identifying the most closely interacting genes in the PPI.

2.6 Survival analysis

We used the clinical data of TCGA, ICGC, OICR and CPTAC PDAC cohorts for survival analysis. We compared the overall survival (OS) between PDAC patients classified based on gene expression levels (high expression levels >mean > low expression levels). Kaplan-Meier survival curves were used to show the survival time differences, and the log-rank test was utilised to evaluate the significance of survival time differences between both groups. We used the R package "survival" to perform survival analysis (57), and the function "coxph" in the R package "survival" was used for the u*nivariate* and *multivariable Cox regression analyses (57)*.

2.7 Evaluation of immune scores, stromal scores, and tumour purity in stromal content

We utilised the "ESTIMATE" R package to calculate an immune score representing the enrichment levels of immune cells and a stromal score representing the content of stromal cells (58) in the TCGA-PDAC cohort. We compared immune and stromal scores between the patients with high expression of *PLAU* and low expression of the *PLAU* group in PDAC (high expression levels >mean > low expression levels). We considered the Wilcoxon sum rank test (P-value ≤0.05) to identify significant differences between both groups.

2.8 Associations of the expression levels of *PLAU* with immune signature, pathway activity, and tumour phenotypes in PDAC

We first identified the *PLAU* correlated cell function and immune gene signatures. Then we used the single-sample gene-set enrichment analysis (ssGSEA) to quantify the enrichment scores of immune and stromal signatures in tumours based on the expression levels of their marker genes (53). We defined the ratio of immune signatures in a tumour sample as the ratio of the average expression levels of their marker genes. The immune and stromal signatures analysed included B cells, CD8+ T cells, CD4+ regulatory T cells, macrophages, neutrophils, natural killer (NK) cells, tumour-infiltrating-lymphocytes (TILs), regulatory T cells (Tregs), cytolytic activity, T cell activation, T cell exhaustion, T follicular helper cells (Tfh), M2 macrophages, tumour-associated macrophage (TAM), T helper 17 cells, myeloid-derived suppressor cell (MDSC), endothelial cell, and cancer-associated fibroblasts (CAFs). Their marker genes are shown in Supplementary Table (ST) B. Moreover, we identified the ssGSEA score of all enriched pathways that directly correlate with *PLAU* and tumour phenotypes (proliferation, EMT, stemness, ECM degradation, and hypoxia). The genes associated with the specific pathways and phenotypes are listed in STB, ST12. Finally, we compared immune signatures and phenotypes of PDAC patients with high expression of *PLAU* with those with low expression of the *PLAU*.

2.9 *In vitro* and *in vivo* study

2.9.1 Isolation and characterisation of cancer-associated hPSCs

Using the outgrowth method (59), CAhPSCs were isolated from surgically removed pancreatic tissue obtained from cancer patients. The characterisation of CAhPSC yield was then assessed by morphology and immunostaining for the selective GFAP and the activation marker αSMA (60).

2.9.2 Cell culture

AsPC-1 cells (American Type Culture Collection, Manassas, VA) and CAhPSCs were cultured according to the supplier's instructions and following previously published protocols by our group (61).

2.9.3 *In vivo* orthotopic model of pancreatic cancer

To validate the outcome of *PLAU* (uPA) inhibition on tumour growth and metastasis *in vivo*, we conducted a pilot study using an orthotopic model of pancreatic cancer as previously established in our laboratory (21, 62, 63). Briefly, 6-8 weeks old female athymic nude mice (BALBc nu/nu) were anaesthetised, and an opening was made in the left flank, followed by exteriorisation of the spleen and tail of the pancreas. Then 1×10^6 human PC cells (AsPC-1) plus 1×10^6 cancer-associated human PSCs (CAhPSCs) in 50μL of PBS were implanted into the tail of the pancreas to replicate early cancer development and progression. Mass Spectrophotometry–Based proteome profiling (ST19) confirmed *PLAU* protein expression in both AsPC1 and CAhPSCs. Seven days after cell implantation, mice were randomised (n=5/group) to receive vehicle control (Ctrl), Gemcitabine (G) 75 mg/kg IP biweekly, uPA small molecule enzymatic inhibitor [5,6-disubstituted amiloride analogue, compound BB2-30F (A26) (64)] 3mg/kg (U3) or 10mg/kg (U10) IP daily. BB230F compounds were formulated for IP injection in 50 mM acetate buffer (pH5.5) + 10% DMSO + 1% Kolliphor HS-15 buffer and filtered through 0.22 μm PVDF syringe-driven filters under sterile conditions (64) The total number of vehicle injections was 28 (daily IP injections), allowing us to control maximally for any effects of IP injections per se in our model. Pancreatic tumour growth was monitored by palpation. At the end of 28 days of treatment, tumours were resected, and tumour volume was determined according to the formula (1/2(length × breadth × width) using digital Vernier callipers (Intech Tools, Thomas Town, VIC, Australia). The abdominal cavity, mesentery, spleen, liver, and lungs were examined, and a metastasis score was calculated based on the presence or absence of visible macrometastatic nodules. Haematoxylin and eosin staining was performed to confirm the presence of such nodules. Primary tumour sections were immunostained for E-cadherin, vimentin and ALDH1A1. Tumour volume data are expressed as mean ± SEM. One-way analysis of variance with Tukey's *post hoc* test was applied. Analyses were performed using GraphPad Prism 9 for Windows 64-bit (GraphPad Software, San Diego, CA, USA).

The animal studies were approved by the University of New South Wales Animal Care and Ethics Committee (Approval Number 18/125B) and accomplished under ARRIVE guidelines.

3 Results

3.1 *PLAU* is significantly differentially expressed in various cancers

Using the GEPIA dataset, it was found that *PLAU* mRNA levels are significantly differentially expressed (compared to relevant normal tissue) in 23 of the 33 different types of cancers assessed (Figure 2A; Red =tumour and Green= normal). In BLCA, BRCA, CESC, COAD, DLBC, ESCA, GBM, HNSC, KICH, KIRC, LGG, LIHC, LUAD, LUSC, OV, PAAD, PRAD, READ, STAD, TGCT, THCA, THYM, and UCEC *PLAU* is significantly upregulated while in KICH, KIRC and PRAD it is downregulated (Figure 2A). In particular, in the PAAD cohort of pancreatic cancer, *PLAU* transcripts were 4.876 (p=1.6e-103) fold elevated compared with normal tissue. In support of the above observations, the Cancer Cell Line Encyclopedia (CCLE) dataset revealed that (https://www.broadinstitute.org/ccle) *PLAU* was also differentially expressed in different cancer cell lines (Figure 2B), including 44 pancreatic cancer cell lines (from primary and metastatic PDAC tumours (ST2 A). Upregulated mRNA and protein expression levels for *PLAU* (relative to normal controls) in 17 PDAC cell lines are depicted in Figure 2C.

The above observations related to PDAC were further confirmed by analysis of several GSE microarrays which showed significant fold increases in *PLAU* mRNA in PDAC vs normal controls as detailed in the following: GSE16515 (logFC 2.73, P=2.32E-07); GSE58561 (logFC 4.94, P = 5.35E-06); GSE71989 (logFC 3.29, P =2.56E-06); GSE62165 (logFC 3.31, P = 1.91E-27); GSE71729 (logFC 1.56, P = 1.98E-09), and RNAseq GSE119794 (logFC 1.256, P= 0.003), ST3. Taken together, the above findings indicate that *PLAU* is significantly upregulated in different tumours and cancer cell lines. Of particular relevance to this study, pancreatic cancer and cell lines, consistently demonstrate upregulation of *PLAU* gene expression, suggesting that *PLAU* may play driver roles in the development and progression of PDAC.

3.2 Upregulated mRNA expression of *PLAU* is associated with poor survival in PDAC patients

Given the significant upregulation of *PLAU* in PDAC patients from distinct datasets, we further investigated the association of *PLAU* with clinical outcomes. TCGA data of 147 PDAC patients from 179 PAAD-TCGA cohorts were
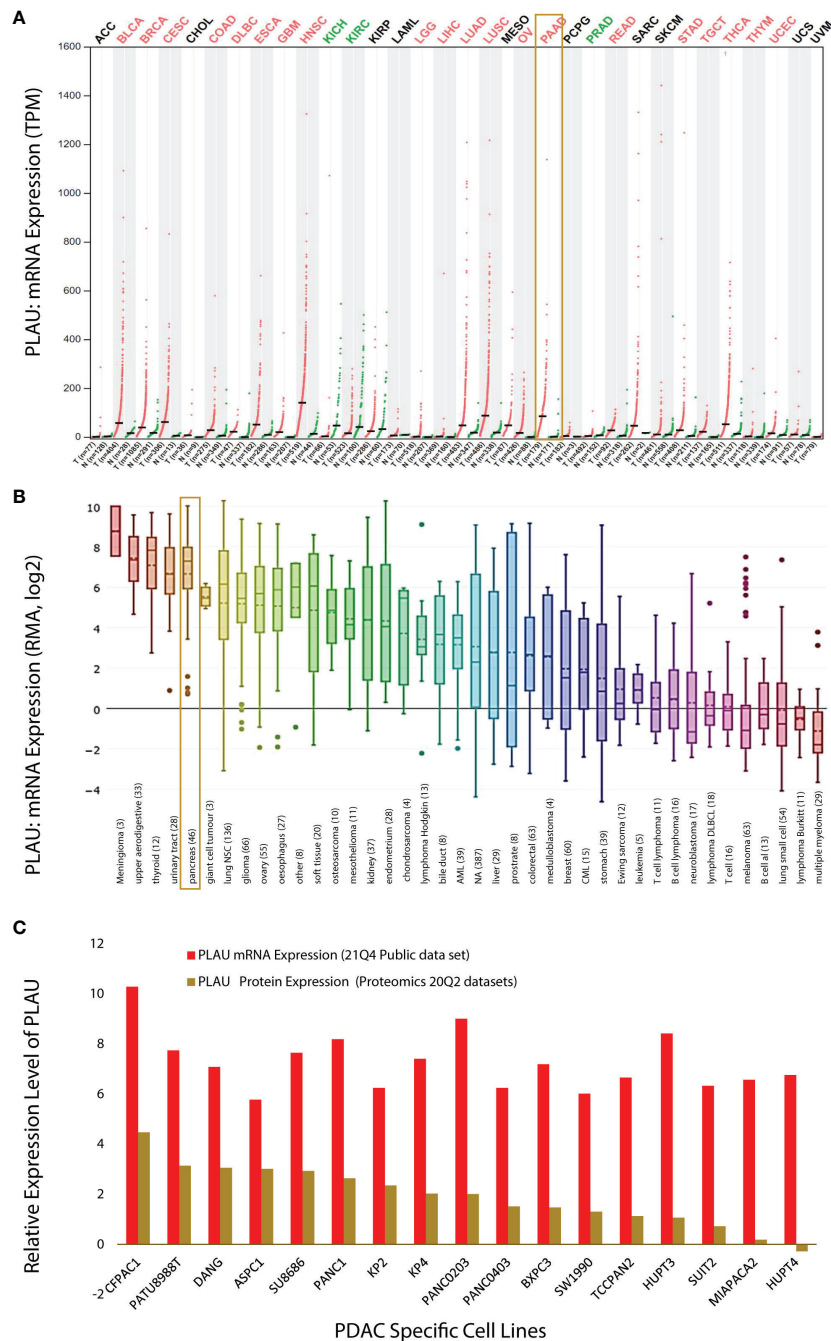
FIGURE 2

PLAU expression in cancers. **(A)** Dot plot depicting *PLAU* gene expression profile across 33 cancer types and paired normal samples (TCGA normal plus GTEx), with each dot representing a distinct tumour or normal sample. The bar height represents the median expression of a certain tumour type or normal tissue. The comparison was performed using GEPIA (Gene Expression Profiling Interactive Analysis). For each TCGA tumour (red), its matched normal and GTEx data (green) are given; T: tumour; N: normal; n: number. Y-axis: transcripts per million log2 (TPM + 1). X-axis: number of tumours and normal samples. **(B)** *PLAU* expression across 1111 human cancer cell lines from the Cancer Cell Line Encyclopedia (CCLE). Box plots showing RNA-seq mRNA expression data from CCLE, with the dashed lines within a box representing the mean. Cell lines derived from the same organ/organ system were grouped, and lineages are indicated at the bottom of the graph, with the number of cell lines per organ/organ system in parenthesis. The "pancreas" group includes the 44 pancreatic cancer cell lines listed in (ST2A). **(C)** Relative expression level of *PLAU* at mRNA and protein level in 17 PDAC cell lines using the depmap portal.

analysed to reveal that patients in the high *PLAU* mRNA expression group had the poorest outcome (high expression group of *PLAU* > mean expression level of *PLAU* > low expression of *PLAU*) (Figure 3A), P=0.042. Similar results were obtained on analysis of the ICGC patient cohort (GSE36924) (Figure 3B), P=0.04 (4). With the third patient cohort in our study (OICR; EGAS00001002543) (65), there was a trend for poorer survival in patients with high *PLAU* mRNA expression, but the difference did not achieve statistical significance P= 0.28 (Figure 3C). Altogether, these data demonstrate that the upregulation of *PLAU* mRNA expression is an adverse prognostic factor in PDAC.

3.3 *PLAU* is significantly correlated with key signal regulatory and tumour immune genes in PDAC

In view of our finding of an association between high *PLAU* gene expression and poor prognosis in PDAC patients, we were interested in analysing other genes that may be correlated with *PLAU* and might influence patient outcomes. Pearson's correlation coefficient test was used to identify gene-gene correlations for all genes in the expression tables of the TCGA, ICGC, and OICR datasets. A Venn diagram was applied to identify *PLAU*-correlated genes common to all three PDAC datasets (ST4, ST5 and Supplementary Figures (SF) 1A, B). The gene signatures were then categorised into different gene families based on annotated gene sets from Molecular Signatures Database (MSigDB). There were 676 genes positively correlated with the *PLAU* that were common to all three datasets. (ST 6A, SF 1A). These included 42 transcription factors (e.g. *FOXC1, HMGA2, RUNX2, SNAI1, SNAI2, TWIST1*, and *WT1*), 16 protein kinases (e.g. *MET, MAPK12*, and *AKT3*), 8 homodomain proteins (including *SIX4, NKX3-2*, and *HLX*);, 27 cell differentiation markers (including *PDL1, CD44, CD70, CDH2*, and *ITGA3)*, 18 oncogenes (e.g. *CDH11,*

COL1A1, and *PDGFB)*, 16 translocated cancer genes (*CDH11, CLTCL1, COL1A1, MAF*, and *MAFB)*, one tumour suppressor gene *WT1, and* 38 cytokines and growth factors (including *TGFB2, FGF1, VEGFC, PDGFB, EREG, TGFB1, CCL11, TGFB3, BMP1, IL1,1* and *CCL13)* [Pearson correlation, r>0.3, P> 0.05].

There were 428 genes negatively correlated with the elevated expression levels of *PLAU* that were common to all three datasets (SF 1B). These comprised 31 transcription factors (including *CDX2, FOXA2, GATA6, HNF1A, HNF4A, PDX1, PPARGC1A*, and *TOX3)*, two cell differentiation markers (*FUT4* and *TNFRSF11A)*, 11 protein kinases (e.g. *ACVR1B, ERBB3, FGFR4, HIPK2, KALRN, PKDCC, SCYL3)*, four translocated cancer genes (including *PRDM16* and *TMPRSS2)*, six oncogenes (including *MYCN, CEBPA*, and *MECOM)*, one tumour suppressor gene (*HNF1A)* and four cytokines and growth factors (including *FAM3B, EDN3, SEMA4G*, and *FAM3D*, ST 6A). Several immune-related gene signatures that are positive and negatively associated with *PLAU* were also identified (such as *PDCD1LG2, HAVCR2, ANXA1, TNFRSF12A, PLAT, CD276, PTGES, CD44, MMP9, CT45A3, PIWIL2, METTL7A, IL23R, IL17RB, IL22RA1, TNFRSF11A, BLNK*, and *F5*, ST7).

Further analysis shows that most of the positively correlated gene signatures of *PLAU* in PDAC regulate cancer cell functions such as cell proliferation, stemness and epithelial-mesenchymal transition, and other factors of importance to cancer biologies such as extracellular matrix degradation, hypoxia, endothelialisation, and metastasis promotion. In contrast, negatively correlated gene signatures were largely uninvolved in cancer cell functions (ST 6C, SF 1E and F).

A subanalysis of TCGA transcriptomic and clinical data of PDAC patients revealed specific gene signatures (positively and negatively correlated with *PLAU*) associated with poor survival (ST8, SF 1C and D). Among these prognostic genes, we further identified the following positively correlated *MET, ITGA3, EREG, PLOD2, EMP1, CD44 HMGA2, TGM2, GAPDH,*
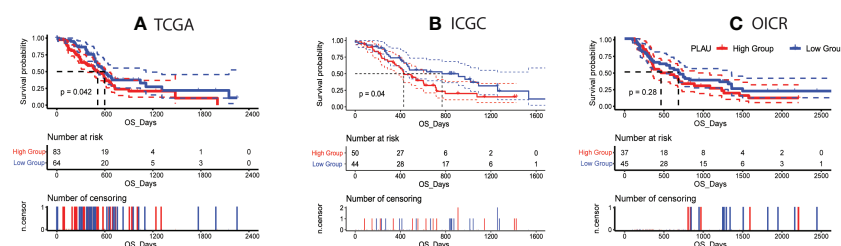

FIGURE 3
Correlation of *PLAU* gene expression with survival in PDAC. **(A, B)** Kaplan-Meier survival curves show that high *PLAU* expression correlated with significantly poorer overall survival (OS) in the TCGA and ICGC PDAC cohorts (log-rank test, P < 0.05), **(C)** but this was not evident with the OICR-PDAC cohort (log-rank test, P = 0.28).

IL31RA, CGB7, CDH3, and negatively correlated *PRDM16, PPARGC1A, CAPN6, SPIB, TOX3*, and *FGFR4* associated with the different cancer cell functions listed in Table 1, while Kaplan Meier curves signifying their prognostic association are presented in Figures 4 and SF 2.

3.4 *PLAU* correlated gene signatures and protein-protein interaction network analysis

The gene analysis described above indicates that upregulated *PLAU* expression is correlated with several key gene signatures that have the potential to influence cancer cell functions and PDAC progression/outcomes. The daunting task is to understand how these positively and negatively *PLAU* correlated genes modulate the PPI network, which can result in dysregulated oncogenic pathways with functional and therapeutic significance. To address this, the 676 positively correlated genes and the 428 negatively correlated genes (common to all three data sets) were entered into the STRING v11 program. 610 of the 676 positively correlated genes and 317 of the 428 negatively correlated genes were involved in the PPI network with PPI enrichment p-value < 1.0e-16 and 3930 edges, and p-value < 1.0e-16 577 edges, respectively. Based on the degree of interactions, some of the top genes within the PPI network were *FN1, GAPDH, COL1A1, CD44, MMP2, COL1A2, MMP9 POSTN, COL5A1, BGN, LOX, COL4A1, MMP14,*

THBS1, and *TGFB1* (ST9A). Extracting the *PLAU*-centric PPI network from the original extensive network revealed that *PLAU* interacts with 31 of the positively correlated genes (*FN1, MMP2, GAPDH, CD44, MMP9, MMP14, SERPINE1, TIMP2, TGFB1, THBS1, CAV1, MET, MMP13, TIMP3, VEGFC, IGFBP3, CTSB, ITGA5, SNAI1, PLAT, CTSL, CTSD, MMP11, ITGA3, PDGFC, MRC2, PRSS23, SRPX2, KAL1, MFI2*, and *LYPD3*, SF3 and ST 9C), and interestingly, only one negatively correlated gene *ANG* (ST 9B, D).

3.5 *PLAU* regulates cancer-associated and metabolic pathways in PDAC

To delineate the specific cancer-associated pathways that may be modulated by *PLAU* and its positive/negatively correlated gene signatures, the Functional Class Scoring (FCS) method based on GSEA tool (53) was used (FDR<0.05). Genes that are positively correlated with *PLAU* upregulation were found to be associated with the enrichment of several cancer-associated KEGG pathways (ST 10A). In order to assess whether the expression of *PLAU* was directly associated with the activity of these pathways, correlations between the expression levels of *PLAU* (Log2 normalised) and the specific pathway activity (ssGSEA score of the pathway) were analysed for the TCGA-PDAC cohort (Spearman's correlation test P<0.05). Interestingly, it was found that *PLAU* expression correlated directly with the activity of 11 KEGG pathways, including

---

TABLE 1 *PLAU* correlated genes and their association with cellular functions in PDAC.

Prognostic genes positively correlated with *PLAU*	Factors influencing cancer biology
HMGA2	Stemness, oncogene, Transcription Factor and Translocating cancer gene
TGM2	Endothelialization, Hypoxia and EMT
CD44	ECM degradation, EMT and Cell differential marker
ITGA3	ECM degradation and cell differential marker and Metastasis
MET	Oncogenes and Protein Kinase
EREG	Cell Proliferation, Cytokines and Growth Factor
GAPDH	Hypoxia
PLOD2	ECM degradation and EMT
EMP1	Cell Proliferation
IL31RA	Cell Proliferation
CGB7	Cytokines and Growth factor
CDH3	Metastasis promotion
Prognostic genes negatively correlated with *PLAU*	**Factors influencing cancer biology**
PRDM16	Oncogenes, Transcription Factors, Translocating cancer genes
PPARGC1A	Hypoxia, Transcription Factor
CAPN6	ECM degradation
SPIB	Transcription Factor
TOX3	Transcription Factor
FGFR4	Cytokines and Growth factor and Protein Kinase

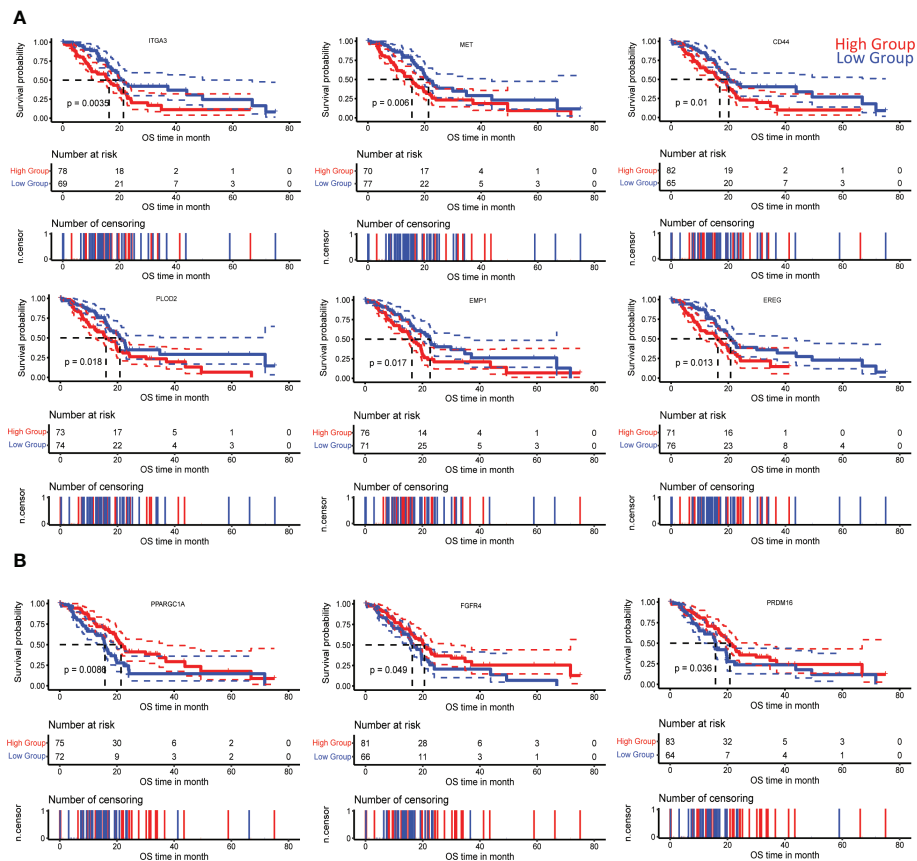ECM, Extracellular matrix; EMT, Epithelial-mesenchymal transitions.

FIGURE 4

Correlation of *PLAU-associated* genes with survival in PDAC. Kaplan-Meier survival curves show that significantly worse overall survival of PDAC patients in the TCGA cohort is correlated with **(A)** increased expression of ITGA3 (log-rank test, P=0.0035), MET (log-rank test, P = 0.006), CD44 (log-rank test, P= 0.01), PLOD2 (log-rank test, P = 0.018), EMP1 (log-rank test, P = 0.017), EREG (log-rank test, P = 0.013) and **(B)** decreased expression of PPARGC1A (log-rank test, P = 0.0086), FGFR4 (log-rank test, P = 0.049), and PRDM16 (log-rank test, P = 0.036).

glycosaminoglycan biosynthesis - chondroitin sulfate, basal cell carcinoma, Hedgehog signalling pathway, axon guidance, pathways in cancer, pancreatic cancer, TGF-beta signalling pathway, arrhythmogenic right ventricular cardiomyopathy (ARVC), wnt signalling pathway, and renal cell carcinoma, FDR<0.01 (Figure 5A and ST 11A).

Genes that were negatively correlated with *PLAU* upregulation were found to be primarily associated with the enrichment of 31 metabolic pathways, covering the metabolism of specific amino acids, carbohydrates, fatty acids and xenobiotics listed in (ST 10B). Interestingly, we discovered that the expression of *PLAU* itself was directly correlated with 25 KEGG pathways (Figure 5B and ST 11B).

A similar observation of *PLAU* association with cancer-associated and metabolic pathways in various cancers, including COAD, HNSC, KIRC, LIHC, BRCA, and LUAD, was revealed in our further analysis (SF 4A, B).

3.6 *PLAU* expression is correlated with pancreatic stellate cell -selective markers & pathways in TME of PDAC

As noted earlier, PSCs facilitate the survival and growth of PDAC cells *via* factors that modulate cancer cell proliferation, invasion, migration, metastasis and chemoresistance. In turn, cancer cells activate PSCs *via* the secretion of growth factors and cytokines (*PDGF, VEGF, bFGF, TGF-ß*), resulting in increased PSC proliferation, migration and production of extracellular matrix proteins (66–69). Given this bidirectional interaction between PSCs and cancer cells, we investigated the association of *PLAU* expression with the abundance of activated PSCs. *PLAU* expression was significantly positively correlated (R= 0.41, P=2.754e-07) with the ssGSEA score of PSC-specific markers in the TCGA-PDAC data set (Figure 6A). Moreover, a significant moderate correlation was found between *PLAU* and all other secreted markers of
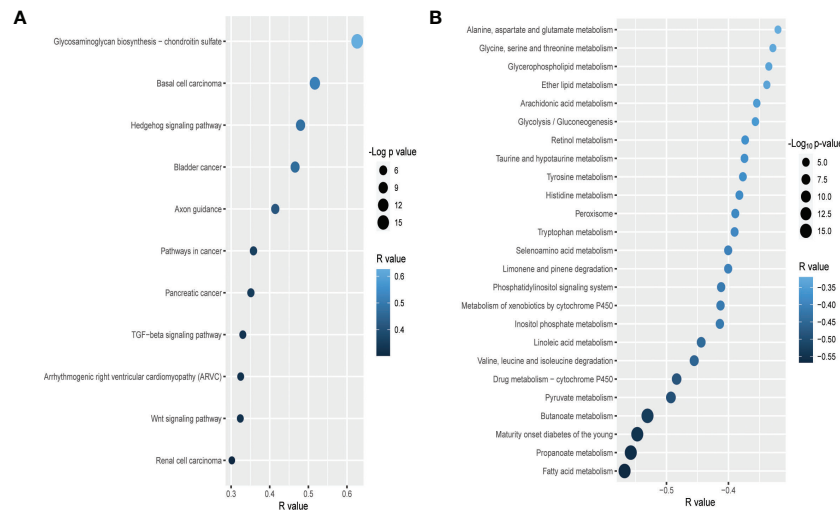
FIGURE 5
Correlation of *PLAU* upregulation with cancer-associated and metabolic pathways in PDAC. In the TCGA PDAC cohort, upregulation of *PLAU* gene expression is **(A)** directly and positively correlated with cancer-associated pathways and **(B)** negatively correlated with metabolic pathways (FDR<0.05).

activated PSCs (ST13), most of which have been shown to play key roles in cancer progression (please see discussion). *PLAU* expression was also correlated with critical pathways known to mediate PSCs-PC interactions (69), including Hedgehog, TGF beta, WNT (Figure 5A), WNT beta-Catenin and hypoxia-inducible factor-1 (Figures 6B, C) signalling pathways.

## 3.7 Identification of prognostically important *PLAU* correlated matrisome gene in human PDAC

In the tumour microenvironment, *PLAU* is involved in ECM breakdown through activation of plasminogen to plasmin which activates certain pro-matrix metalloproteinases, facilitating local tumour invasion. Dysregulated ECM proteins also influence tumour progress and patient survival by supporting tumour cell proliferation, angiogenesis, inflammation (22, 28), and metastasis (29, 30). However, the association of *PLAU* with the PDAC-specific matrisome gene (produced by tumour cells and stromal pancreatic stellate cells) has not been assessed in the context of PDAC development and progression. In order to systematically examine the correlations of *PLAU* expression with PDAC-specific ECM gene signatures (from TCGA, ICGC and OICR cohorts), 155 PDAC matrisome gene signatures (ST14) were selected (32 secreted by cancer cells, 87 by stromal cells and 36 from both cancer and stromal cells) (70). 49 ECM gene signatures were found to be correlated with *PLAU*, either positively (33) or negatively (3) (Pearson correlation, *r>0.3; p< 0.05*). Of the 49 genes, 22 coded for ECM glycoproteins (*EFEMP1, EMILIN1, FBLN2, FBN1, FN1,*

HMCN1, IGFBP3, LAMA4, LAMC2, LTBP1, LTBP2, MATN2, MFAP2, PCOLCE, POSTN, PXDN, SRPX2, TGFBI, TGM2, THBS1, THBS2 and *TNC*), 12 for ECM regulators (*ADAMTS4, ADAMTSL1, BMP1, CTSB, CTSD, LOX, LOXL1, MMP2, PLOD1, PLOD2, SERPINH1* and *TGM2*), six for collagens (*COL11A1, COL6A1, COL6A2, COL6A3, COL8A1,* and *COL8A2*), four for ECM-affiliated proteins (*ANXA1, ANXA4, LGALS1* and *LGALS4*), three for secreted factors (*S100A16, S100A9,* and *TGFB1*), and two for proteoglycans *BGN* and *VCAN* (ST14, 15A and Figure 7A).

Survival analysis of the TCGA-PDAC cohort revealed that secreted factor *S100A16 (*cancer-cell–derived), ECM regulator *PLOD2 (*stromal cell-derived) and ECM regulator *TGM2 (*derived from both cancer cells and stromal cells) genes were overexpressed in human PDAC and correlated with short patient survival (log-rank test, P < 0.05), Figures 7B–D. In contrast, none of the negatively correlated matrisome gene signatures was associated with patient survival. However, at the protein level (using the CPTAC-PDAC cohort), while PLOD2, S100A16 and TGM2 were all significantly differentially overexpressed in tumours compared to the normal adjacent pancreas (ST 15B), only upregulation of PLOD2 (log-rank test, P= 0.05) protein was found to be associated with poor survival (refer to PLOD2).

3.8 Upregulation of the *PLAU* gene is correlated with aggressive phenotypes of PDAC

Aggressive PDAC is characterised by increased cancer cell proliferation, EMT, stemness, active ECM and hypoxia. Using
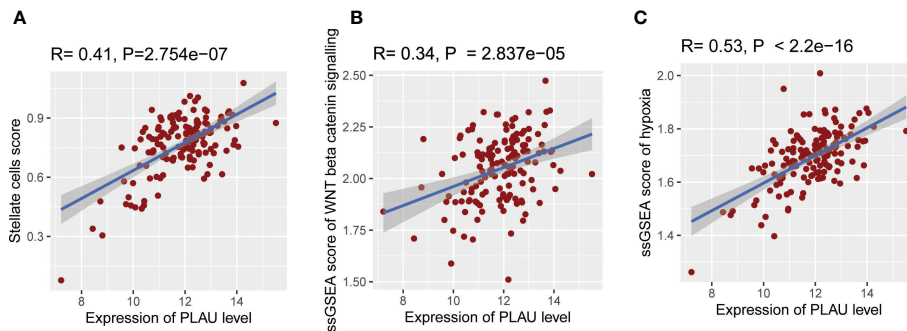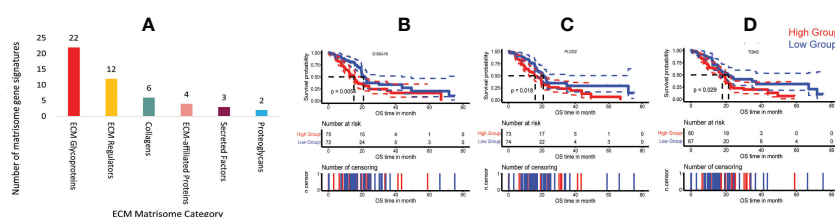
FIGURE 6

Association of *PLAU* gene expression with abundant activated PSCs and pathways responsible for PSC-PC interactions. In the TCGA PDAC cohort, **u**pregulation of *PLAU* gene expression exhibit a significant positive association with **(A)** abundance of activated PSCs in the TME (R= 0.41, P=2.754e−07), **(B)** WNT beta-Catenin pathway activity (R= 0.34, P=2.837e−05), and **(C)** hypoxia score (R= 0.53, P < 2.2e−16).

the TCGA-PDAC cohort to compare the *PLAU* high expressing group (HEG) vs the *PLAU* low expressing group (LEG), scores for each of the above parameters were found to be elevated (Figures 8A–E), and the associated markers significantly correlated (SF 5A–D) with high *PLAU* gene expression.

3.9 Expression of the *PLAU* gene is associated with an immunosuppressive tumour microenvironment in PDAC

Since the infiltration levels of immune cells are an independent predictor of survival in cancers (58), the differences in various immune and stromal signatures between *PLAU*-high and *PLAU*-low patients in the TCGA-PDAC cohort were examined. Stromal and immune scores were calculated (the content of cells) by applying the ESTIMATE (58) algorithm. The stromal score was significantly higher in the HEG of *PLAU* than in the LEG of *PLAU* (Figure 9A, Wilcoxon rank-sum test, p<0.05). In contrast, there was no significant difference in the immune score between the groups. However, the *PLAU*-high

group was associated with inhibition of immune stimulatory signatures that included CD8+ T cells, NK cells, and type 2 IFN (Figure 9B) and upregulation of immunosuppressive signatures that included CAFs, macrophages, cancer-testis antigens, PI genes, *PD-L1*, *PDL-2*, and *TGFB1* (Wilcoxon rank-sum test, p<0.05) (Figure 9C). The ratios of CD8+ T cells/CD4+ T cells and pro-/anti-inflammatory cytokines (as assessed by the ratio of average expression levels (log2-transformed) of their marker genes) were significantly lower in the *PLAU* high group (expression levels > average) (Figure 10A, P < 0.05). The pro-inflammatory cytokine genes are immune-stimulatory and include *IFNG*, *IL-1A*, *IL-1B*, and *IL-2*, while the anti-inflammatory cytokine genes *IL-4*, *IL-10*, *IL-11*, and *TGFB1* represent an immune-inhibitory signature. The expression levels of *PLAU* were negatively correlated with CD8A/PD-L1 and CD8A/PD-L2 ratios (Pearson's correlation test, P < 0.05, Figure 10B). Taken together, the above findings indicate that elevated *PLAU* expression has a stronger association with immunosuppressive TME signatures (*PD-L1* and *PD-L2*) than with the anti-tumour immune signature (CD8+ T cells) in the TCGA-PDAC cohort.

FIGURE 7

Correlation of *PLAU* expression and matrisome gene signatures in human PDAC. **(A)** Upregulation of *PLAU* gene expression was positively correlated with various PDAC ECM matrisome gene signatures. Kaplan Meier survival curves show that in the TCGA-PDAC cohort, poor survival was associated with **(B)** increased expression of *S100A16*, P = 0.0054, **(C)** *PLOD2*, P = 0.018 and **(D)** *TGM2*, P=0.029.
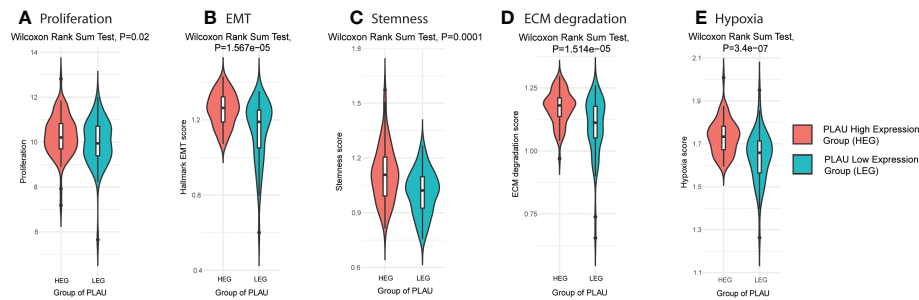
FIGURE 8

PLAU upregulation is associated with aggressive phenotypes of PDAC. Markers of an aggressive phenotype of PDAC were positively correlated with the high *PLAU* expressing group (HEG) compared to the low *PLAU* expression group (LEG), as depicted for **(A)** the tumour cell proliferation and growth index marker, MKI67, Wilcoxon rank–sum test, P= 0.02 **(B)** EMT Wilcoxon rank–sum test, P= 1.567−05, **(C)** tumour stemness, Wilcoxon Rank Sum Test, P=0.0001, **(D)** ECM degradation, Wilcoxon Rank Sum Test, P= 1.514e−05 **(D, E)** hypoxia, Wilcoxon Rank Sum Test, P= 3.4e−07.

3.10 *PLAU*-correlated prognostic gene markers are also differentially expressed and associated with poor outcomes in PDAC at the protein level

In order to determine whether the identified prognostic gene signatures (*PLAU* correlated 41 positively and 34 negatively in the TCGA-PDAC cohort) translated to protein or not in the PDAC tumour, we performed a differential expression analysis based on the CPTAC-PDAC cohort. 135 patients' tumours proteome profile compared with proteins expression data from 67 normal adjacent and nine normal ducts tissues. The results showed that 23 out of 41 positively correlated prognostics markers were differentially upregulated; out of 34 negatively correlated prognostics markers, 16 were differentially downregulated (ST17).

The correlation of the differentially expressed protein signatures noted above with overall patient survival was also assessed in the CPTAC-PDAC cohort. Upregulated expression of CD44, CDH3, FNDC3B, HMGA2, ITGA3, MET, PPP1R14B, and PLOD2 and downregulation of KIAA0513, OTC, and LYZ were associated with poor survival (Figures 11A, B). Representative immunohistochemistry images from the human proteome atlas further confirmed the level of expression of the above proteins in PDAC tissues (71) (SF6).

3.11 Univariate and multivariate cox regression analysis of *PLAU* correlated (survival-related) proteins and different clinicopathological factors

To rule out the bias caused by the survival-related clinical parameters in the following analysis, we obtained the clinical dataset from CPTAC-PDAC and screened for the survival-related clinical index by univariate and multivariate cox regression analysis. Univariate Cox regression analyses of the CPTAC-PDAC clinical dataset identified eight proteins (out of the 12) and weight, histological grade, distant metastasis, tumour stage, residual tumour, and tobacco smoking history as individual prognostic factors (Figure 12A). Multivariate Cox regression analysis demonstrated that three prognostic proteins (*PLAU*, ITGA3, and PPP1R14B expression) and two clinicopathological factors (tumour stage and tobacco smoking history) were significantly associated with poor survival (Figure 12B).

3.12 *PLAU* and correlated signatures are associated with the basal subtype of PDAC

Identifying the subtypes of pancreatic cancer could assist with providing the patient with a more accurate prognosis prediction and may also allow precise and effective therapy. Therefore, the association of upregulated *PLAU* protein with survival in patients bearing tumours of PDAC basal and classical subtypes was explored (6). The basal/squamous subtype is characterised by mainly low expression of GATA6 with gene signatures enriched for the inflammation, hypoxia response, metabolic reprogramming and TGF-β signalling, and is also characterised by resistance to chemotherapy and poor outcomes. On the other hand, the classical subtype is characterised by high expression of *GATA6*, KRAS dependency, chemoresponsiveness and a better clinical outcome (4, 72). Using the CPTAC-PDAC cohort, we found that upregulation of *PLAU* protein was associated with poor survival (Figure 13A, P=0.0044). Further, a comparison of the survival outcome in basal vs classical clearly shows that the basal group of patients is more at risk of poor prognosis than the classical type (Figure 13B). Assessment of *PLAU* protein expression in basal and classical types
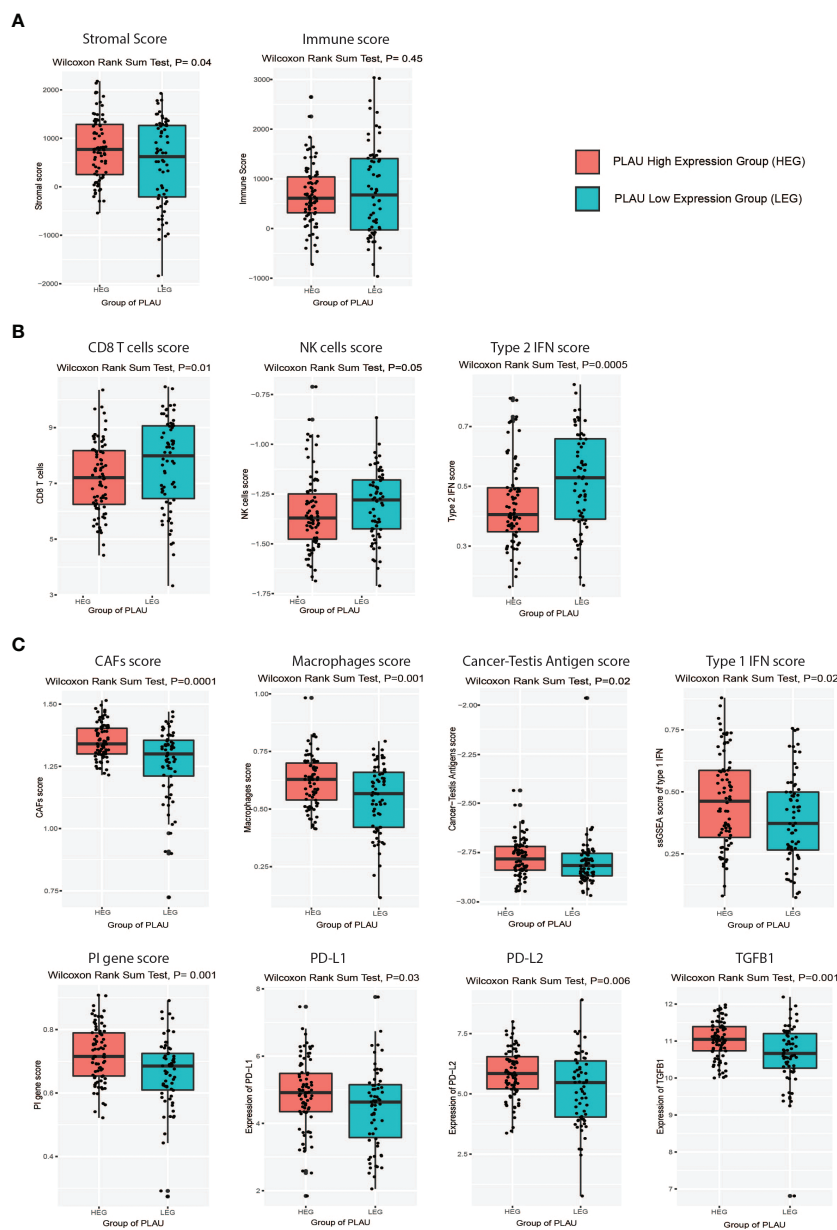
Association of *PLAU* upregulation with an immunosuppressive landscape in the TCGA PDAC cohort. Markers of an immunosuppressive landscape in PDAC were positively correlated with the high *PLAU* expressing group (HEG) compared to the low *PLAU* expression group (LEG), as evidenced by **(A)** a high stromal score (Wilcoxon rank-sum test, P=0.04) and a low immune score (Wilcoxon rank-sum test, P=0.45), **(B)** low scores for immune stimulatory signatures CD8+ T cells (Wilcoxon rank-sum test, P=0.01), NK cells (Wilcoxon rank-sum test, P=0.05), and type 2 IFN (Wilcoxon rank-sum test, P=0.0005), **(C)** high scores for immune inhibitory signatures including CAFs (Wilcoxon rank-sum test, P=0.0001), macrophages (Wilcoxon rank-sum test, P=0.001), cancer-testis antigens (Wilcoxon rank-sum test, P=0.02), Type 1 IFN (Wilcoxon rank-sum test, P=0.02), PI genes (Wilcoxon rank-sum test, P=0.001), PD-L1(Wilcoxon rank-sum test, P=0.03), PDL-2(Wilcoxon rank-sum test, P=0.006), and TGFB1 (Wilcoxon rank-sum test, P=0.001).

demonstrated that *PLAU* was significantly more expressed in the basal group than in the classical type (log2FC=0.80, p<0.001, Figure 13C). Furthermore, in all three PDAC cohorts (TCGA, ICGC and OICR PDAC cohorts), high *PLAU* gene expression was positively correlated with basal markers including *S100A2*

(R=0.48, p=4.57E-10), *FAM83A* (R=0.55, p= 4.38E-13), *IGTA3* (R=0.45, p= 1.14E-08), *KRT5* (R=0.45, p= 6.81E-09), and *C16orf74* (R=0.64, p= 2.48E-18) and negatively correlated with classical molecular subtype markers including *GATA6* (R=-0.57, p= 2.93E-14) *TFF2* (R=-0.42, p= 1.20E-07), *REG4* (R=-0.40, p=

FIGURE 10

Association of *PLAU* upregulation with the immune ratios in the TCGA PDAC cohort. **(A)** CD8+ T cells/CD4+ T cell (P= 0.003) and pro-/anti-inflammat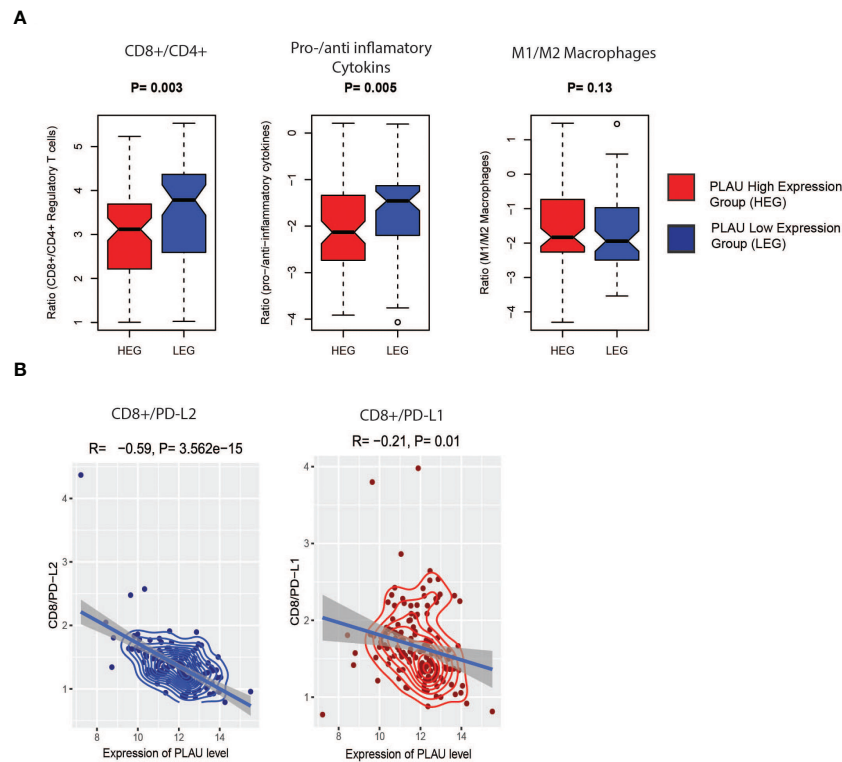ory cytokines (P= 0.005), significantly lower in the high expression group (HEG) of PLAU and **(B)**, the PLAU expression is negatively correlated with CD8A/PD-L1 (Pearson's correlation R=-0.59, P= 3.562e-15) and CD8A/PD-L2 (Pearson's correlation R=-0.21, P= 0.01).

5.98E-07), *LGALS4* (R=-0.39, p= 7.45E-07), and *DDC* (R=-0.44, p= 2.22E-08) (4, 6, 73, 74) (ST 18). Of note, survival analysis in the basal group patients demonstrated poor survival outcomes when stratified into the *PLAU* high group compared to the *PLAU* low group (Figure 13D, P=0.018). Further survival analysis between *PLAU* high basal versus *PLAU* high classical shows that even though upregulation of *PLAU* is found in both basal and classical group patients, *PLAU* high basal is worse than *PLAU* high classical (SF7B, P<0.0001). Consequently, the high and the low in the classical group patients demonstrated no significant association with poor survival (SF7A, P=0.9). These results support the concept that upregulation of *PLAU* protein is clinically associated with the poorest survival outcomes in the basal subtype of PDAC.

3.13 Effect of uPA - inhibition and Gemcitabine on tumour volume and metastasis *in vivo*

Finally, we assessed the effects of uPA inhibition on tumour growth and metastasis using the uPA inhibitor BB230F at 3mg

(U3) and 10mg (U10)/kg body weight alongside the standard of care drug gemcitabine in an early intervention orthotopic xenograft mouse model of pancreatic cancer (Figure 14A). In this model, we observed that uPA inhibition (with U10) was comparable to Gemcitabine in reducing primary tumour volume at the endpoint. Importantly, uPA inhibition was significantly superior to Gemcitabine in reducing liver metastasis (key site in this model), with U10-treated mice showing no evidence of metastasis (Figures 14B, C, SF9A-B and ST20) in the liver. The absence of liver metastases in all animals treated with U10 was confirmed by histology. Since one of the main mechanisms underlying metastasis is increased EMT of cancer cells, we measured EMT in the model by assessing the ratio of expression of the mesenchymal marker vimentin to the epithelial marker E-Cadherin. An increase in the vimentin: E-cadherin ratio is an indicator of increased EMT. In the orthotopic tumours in this model, we found that while vimentin expression was unchanged, E-cadherin expression was significantly elevated in U10-treated mice compared to the other groups in Figures 14D-F, suggesting inhibition of cancer cell EMT by *PLAU* inhibition. We support these observations using the CPTAC-PDAC cohort, whereby patients in the upper
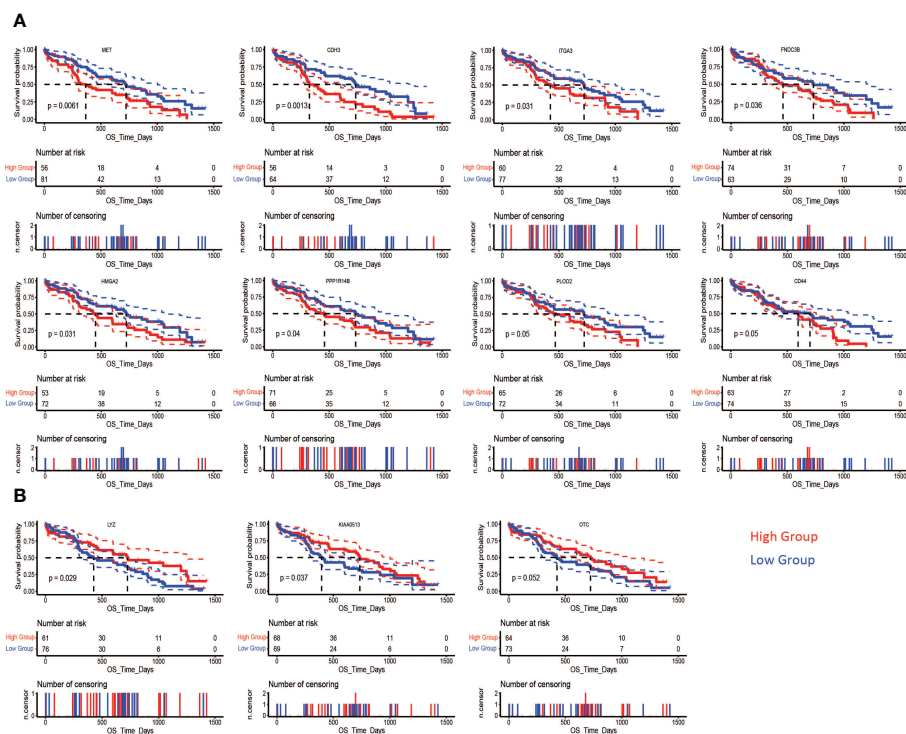
FIGURE 11

Association of differentially expressed proteins and survival in PDAC. In the CPTAC-PDAC cohort, Kaplan-Meier analysis shows that poor overall survival (OS) was correlated **(A)** high expression of MET (log-rank test, P= 0.0061), CDH3 (log-rank test, P= 0.0013), ITGA3 (log-rank test, P= 0.031), FNDC3B (log-rank test, P= 0.036), HMGA2 (log-rank test, P= 0.031), PPP1R14B (log-rank test, P= 0.04), and PLOD2 (log-rank test, P= 0.05) CD44 (log-rank test, P= 0.05), and **(B)** low expression of LYZ (log-rank test, P= 0.029), KIAA0513 (log-rank test, P= 0.037), and OTC (log-rank test, P= 0.05).

quartile of the *PLAU* expression group exhibited a significant decrease in E-cadherin and an increase of vimentin compared to patients in the lower quartile of the *PLAU* expression group (Figures 14G, H). Furthermore, immunostaining for the stem cell marker ALDH1A1, which plays a role in recurrence, metastasis, and treatment resistance, demonstrated that U10 significantly decreased ALDH1A1 expression compared to the mice treated with control and Gemcitabine alone (SF8A, B), suggesting that the uPA inhibition may inhibit cancer stemness.

4 Discussion

Pancreatic ductal adenocarcinoma (PDAC) is an overly aggressive cancer with very high recurrence rates and the poorest prognosis of all solid malignancies. The early and rapid development of metastasis (often seen before the detection of a sizeable pancreatic mass) is the primary driver of the poor clinical outcome of this cancer (75–78).

uPA and its cell surface receptor uPAR play a role in multiple stages of tumorigenesis, especially cancer progression (e.g., ECM degradation and EMT) (7, 24–27, 33–41). Moreover, clinical

evidence demonstrates that high *PLAU* mRNA expression is associated with significantly worse clinicopathological characteristics and poor prognosis in PC patients (79, 80). In this study, we have elucidated the key molecular pathways modulated by or associated with *PLAU* upregulation. This will not only enable better prediction of clinical outcomes but importantly may help stratify and identify patients who may best benefit from therapeutic targeting of the uPA.

Using TCGA, CCLE and GEO databases, we have convincingly demonstrated that *PLAU* mRNA levels were significantly upregulated in 44 PDAC cell lines derived from primary or metastatic tumours compared to normal tissues. Importantly, analysis of the TCGA and ICGC PDAC cohorts confirmed the prognostic value of *PLAU* in pancreatic cancer. Validation of this finding at the protein level was obtained by analysis of the CPTAC-PDAC cohort, which demonstrated that high *PLAU* protein expression was significantly correlated with poor survival in PDAC patients.

To help understand the mechanisms mediating *PLAU*-associated poor survival, gene signatures that were commonly positively or negatively correlated with *PLAU* upregulation were identified in the TCGA, ICGC and OICR PDAC-specific
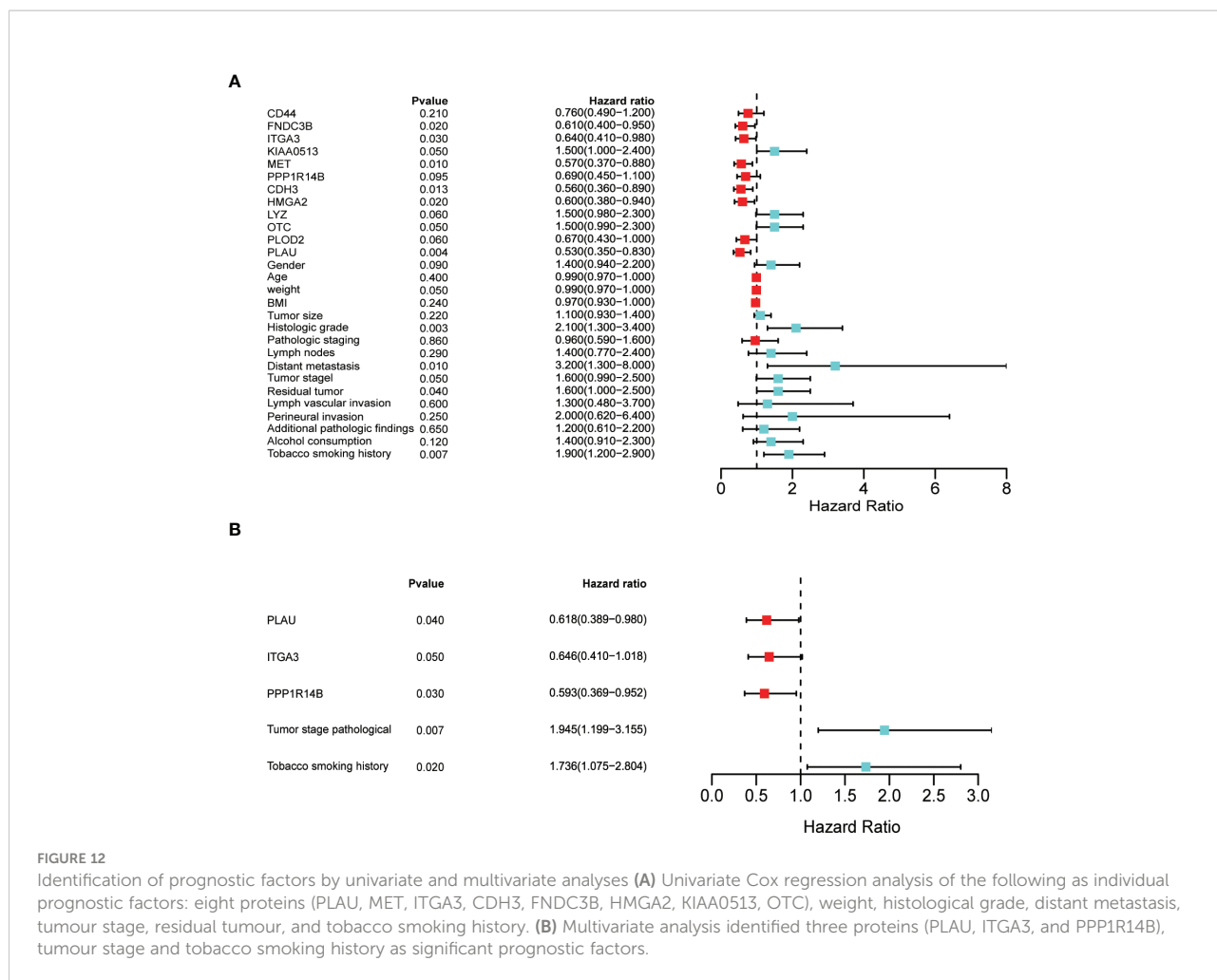
FIGURE 12
Identification of prognostic factors by univariate and multivariate analyses **(A)** Univariate Cox regression analysis of the following as individual prognostic factors: eight proteins (PLAU, MET, ITGA3, CDH3, FNDC3B, HMGA2, KIAA0513, OTC), weight, histological grade, distant metastasis, tumour stage, residual tumour, and tobacco smoking history. **(B)** Multivariate analysis identified three proteins (PLAU, ITGA3, and PPP1R14B), tumour stage and tobacco smoking history as significant prognostic factors.

cohorts. Analysis of these correlated genes revealed that *PLAU* upregulation was associated with gene signatures mainly encoding transcription factors, cytokines, growth factors, protein kinases and oncogene, which are involved with epithelial-mesenchymal transition, ECM degradation, cell proliferation, hypoxia, angiogenesis, stemness and metastasis. Survival analysis revealed that in the TCGA-PDAC cohort, 6% of positive and 7% of negatively correlated gene signatures were associated with poor survival. The key genes and their functions are summarised in Table 1. Of the downregulated genes in colon (81) and ovarian (82) cancer, *PPARGC1A* was reported as a tumour suppressor, and downregulation is associated with poor survival in colon cancer (83). However, the significance of the remaining downregulated genes in PDAC prognosis needs to be explored.

Examination of the protein-protein interaction network revealed that PLAU interacted directly with 31 positively correlated signatures that are active in oncogenesis hypoxia, proliferation, ECM degradation and EMT. On the other hand, PLAU interacted directly with one negatively correlated gene,

ANG (angiogenin), the high expression of which is reported to be favourable in pancreatic cancer (84).

Gene set enrichment analysis confirmed that *PLAU* and its positively correlated signatures were involved with pathways that play a role in cancers. In contrast, *PLAU* and its negatively correlated signatures were predominantly related to the downregulation of metabolic pathways. With respect to the former group, 11 main pathways were identified, as depicted in Figure 5. Of particular interest are the following: i) the Hedgehog signalling pathway - known to be involved in early pancreatic cancer tumorigenesis (85). A component of this pathway Sonic HH (SHH), is increased more than 40-fold in pancreatic cancer stem cells responsible for tumour recurrence (86, 87). Li et al. showed that hypoxia-induced ROS production increases the expression of *PLAU* and MMP2 in pancreatic cancer cells through the Hh signalling pathway to facilitate invasion and metastasis (88). ii) the metabolic pathway glycosaminoglycan biosynthesis - chondroitin sulfate that facilitates invasiveness of cancer cells by supporting the adhesion of various cells such as fibroblasts or leukocytes in
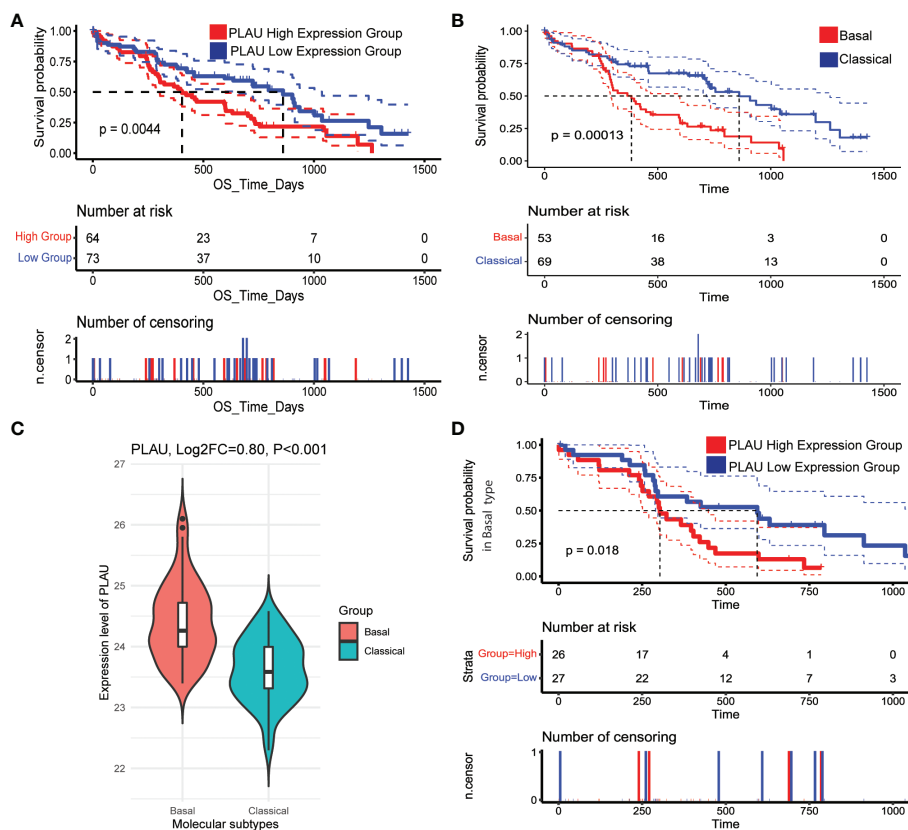
FIGURE 13

PLAU upregulation is associated with the basal type of PDAC. **(A)** In the CPTAC-PDAC cohort, **(A, B)** Kaplan-Meier survival curves show that increased PLAU protein expression is associated with poor prognosis (log-rank test, P=0044), and the basal subtype of PDAC is associated with worse survival than the classical subtype. **(C)** PLAU protein is significantly upregulated in the basal group than classical subtype (Log2FC=0.80, P<0.001); and **(D)** within the basal subtype, the clinical outcome in the high PLAU expression group is significantly worse than the low PLAU expression group (log-rank test, P=0.018).

the TME which are the source of growth factors and ECM-degrading enzymes that enable local migration and dissemination of cancer cells (89, 90). Interestingly, upregulation of components of this pathway, chondroitin and dermatan sulfate, has been reported in pancreatic tumours (91). iii) the Wnt signalling pathway, one of the critical cascades regulating development and stemness in cancer (92). This pathway is known to be critical to the initiation and progression of PDAC (93). iv) the TGF-beta signalling pathway which is most significantly involved in EMT induction in pancreatic cancer cells through activation of ERK/MAPK, PI3K, p38, JNK, RhoA, and other signalling pathways (36–38).

Intriguingly, *PLAU* upregulation and its negatively correlated gene signatures were found to be associated with the downregulation of a large number of metabolic pathways. Such downregulation could be attributed to a severely hypoxic environment in the tumour as a result of pronounced desmoplasia that limits oxygen diffusion (94, 95). Indeed, we

found a significant increase in hypoxia in the high expression group of *PLAU* (Figures 6A, C and 8E). Given the central role of PSCs in the production of desmoplasia, it was also of interest that a significant correlation was identified between *PLAU* upregulation and activated PSC abundance (R= 0.41, P=2.754e-07) as well as between *PLAU* upregulation and Hypoxia-inducible factor-1α expression (R= 0.53, P<2.2e-16), a known PSC activation factor.

Moreover, PLAU upregulation is negatively associated with these pathways, suggesting that downregulation of critical metabolic pathways in pancreatic cancer patients may result in worse outcomes. Evidence suggests that metabolic disorders and failure of immunosurveillance to prevent malignancies are key drivers of cancer progression. The tumour immune escape phenomenon can be induced by several factors, including the loss of antigenicity, the loss of immunogenicity, and the immunosuppressive tumour microenvironment (TME), which are orchestrated by nutrient limitation and the build-up of specific metabolites and signalling molecules (96, 97).
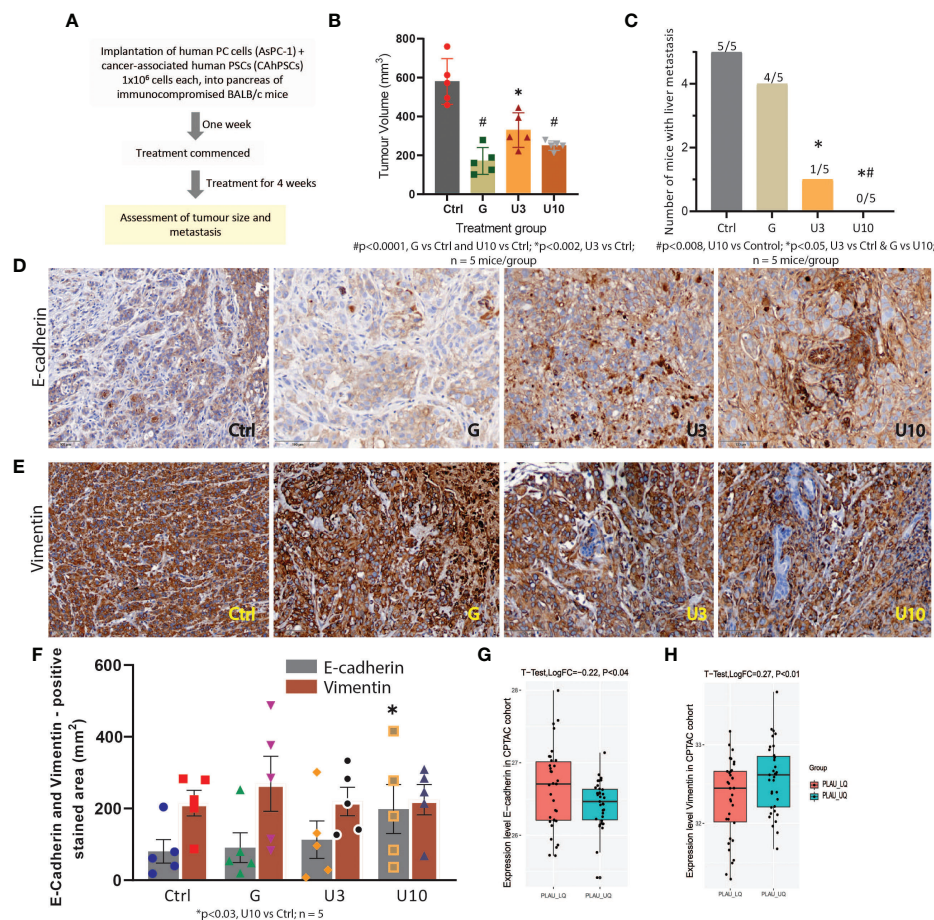
FIGURE 14

In vivo study to assess the effects of PLAU/uPA inhibition and Gemcitabine on tumour progression in an orthotopic model of pancreatic cancer **(A)** Flowchart depicting study design for the orthotopic model. **(B)** Effects of Gemcitabine **(G)**, uPA inhibitor BB230F 3 and 10 mg/kg body weight (U3) (U10), respectively, on endpoint primary tumour volume. Mice bearing orthotopic pancreatic tumours received G, 75 mg/kg body weight twice weekly or U3 or U10 by daily intraperitoneal injections for 28 days. Both gemcitabine and uPA inhibitors significantly reduced tumour volume (n = 5 mice/group). **(C)** uPA inhibition significantly reduced (U3) or completely abolished (U10) liver metastases in mice, while Gemcitabine did not have any effect on metastasis compared to untreated controls. (n = 5 mice/group). **(D, E)** Immunostaining for the mesenchymal marker vimentin and epithelial marker E-Cadherin. Representative photomicrographs depicting staining for E-cadherin and vimentin in mouse pancreas. **(F)** Morphometric analysis shows that while vimentin expression was unchanged by the treatments, E-cadherin expression was significantly increased in U10 compared to controls (n = 5 mice/group). E-cadherin and vimentin (EMT markers), scale bars = 100 µm. **(G, H)** In the CPTAC-PDAC cohort, protein expression analysis of EMT markers indicates that patients in the upper quartile of PLAU expression exhibit low E-cadherin (T-test, LogFC=-0.22 P=0.018) and high vimentin levels (T-test, LogFC=0.27 P<0.01) compared to lower quartile group, suggesting increased EMT in the tumours with upregulated PLAU expression.

The activation of the uPA/uPAR system has been reported to drives aerobic glycolysis (Warburg effect) in melanoma cell lines even in normoxic conditions, and this activation depends on the α5β1-integrin-mediated uPAR connection with EGFR with the engagement of the PI3K-mTOR-HIFα pathway (98). It has been established that the transcription factor HIF-1α promotes aerobic glycolysis and regulates tumour invasion and metabolism (99). Moreover, in this energy-deprived milieu, *PLAU* upregulation was also found to induce more hypoxia and activate the TGF beta pathway, thereby further increasing tumour immune suppression. Based on the above, it would be

reasonable to speculate that uPA may participate in altering and/or downregulating metabolic pathways and in facilitating an immunosuppressive environment, thereby ultimately enhancing tumour progression.

PLAU upregulation was also associated with other PSC-derived factors and pathways that are thought to mediate the well-established bidirectional interaction between PSCs and PDAC cells. Activated PSCs markers that were positively correlated with *PLAU* (Pearson correlation test R>0.30, P<0.05), including *CDH11* [Cadherin-11 is elevated in PSCs and is related to PC cells migration (100)), *MME* (or CD10+

PSCs augment the aggressiveness of PDAC (101)], *LGALS1* [Galectin-1 plays role in the development and maintenance of an immunosuppressive microenvironment and promotes PDAC cells metastasis (102–104)], *FERMT2* [progression of pancreatic cancer (105)), *S100A4* (mesenchymal markers increased in activated PSCs (106)], *TGFb1* [TGF-beta signalling in activated PSCs promote ECM accumulation, induced EMT etc. (107, 108)], *POSTN* [promote cancer cell survival, EMT, invasion, and metastasis (109, 110)], *Runx2* [regulate the transcription of extracellular matrix modulators *SPARC* and *MMP1* and impact the tumour microenvironment (111)], *IL-1*[immune suppression (112, 113)], *IL8* (crosstalk with endothelial cells (20)), *PGDF* (proliferation and angiogenesis (20, 114)) and *PLOD2* (creates a permissive microenvironment for migration of cancer cells (115)).

The prominent ECM in PDAC not only supports cancer progression by directly promoting cellular transformation and metastasis but also affects the function of stromal cells to induce angiogenesis and inflammation, thereby resulting in a pro-tumorigenic microenvironment (116, 117). ECM proteins have also been recognised as essential components of the metastatic niche to maintain cancer stem cell properties and enable the outgrowth of metastasis-initiating cells (118–120). Therefore, an analysis of the association of *PLAU* and specific ECM markers and their prognostic significance was also undertaken in this study. 49 ECM gene signatures were found to be correlated with *PLAU*, of which three, namely, secreted factors *S100A16* (cancer-cell–derived), ECM regulator *PLOD2* (PSC-derived) and ECM regulator *TGM2* (cancer and stromal cell-derived) were significantly associated with poor survival in the TCGA-PDAC cohort. However, survival analysis using the CPTAC cohort revealed that only PLOD2 protein upregulation was significantly associated with poor survival (Figure 11A, PLOD2).

The immune system is now recognised to play a central role in cancer biology. There have been no studies to date assessing the association between *PLAU* expression and immune signatures in PDAC. This study has shown for the first time that *PLAU* expression correlates closely with immune gene signatures in three PDAC cohorts. In fact, upregulation of *PLAU* was associated with immune inhibitory rather than immune-stimulatory signatures. This concurs with the observed association of *PLAU* with growth factors and cytokines known to promote an immunosuppressive tumour microenvironment.

In view of the positive association discussed above between *PLAU* and its correlated signatures and factors that signify tumour aggressiveness, high and low *PLAU* groups in the TCGA-PDAC cohort were analysed. The results confirmed that tumours of patients with high *PLAU* gene expression also exhibited significantly increased proliferation, EMT, stemness, ECM degradation, hypoxia and immunosuppressive TME. These results suggest that *PLAU* and its correlated signatures induce an aggressive cancer phenotype leading to poor survival.

As outlined above, this study has clearly established that dysregulated *PLAU* and its correlated gene signatures have the potential to confer a poor prognosis for PDAC. However, without knowledge of related changes in the proteome, the usefulness of prognosis prediction based on only gene expression remains a challenge. Proteins are the key functional drivers of cancer biology, providing a link between genotype and phenotype and are common targets of anticancer drugs. Thus it is important to note that, using the CPTAC-PDAC cohort, most of the *PLAU* correlated prognostic gene markers identified in the TCGA-PDAC cohort were also found to be differentially expressed at the protein level. Eleven proteins were associated with poor survival, including upregulated CD44, CDH3, FNDC3B, HMGA2, ITGA3, MET, PPP1R14B, and PLOD2 and downregulated KIAA0513, OTC, and LYZ. We further confirmed their expression level in HPA. Out of 11 ITGA3, MET, FNDC3B, PPP1R14B and KIAA0513, including *PLAU*, were previously reported as individual prognostic markers in the pancreatic cancer TCGA-PAAD cohort (84). However, we have shown these for the first time in PDAC as prognostic markers in our analysis at the transcriptome and proteome levels.

Univariate analysis showed that *PLAU*, CDH3, FNDC3B, HMGA2, ITGA3, MET, KIAA0513, OTC, weight, histological grade, distant metastasis, tumour stage, residual tumour, and smoking are individual prognostic factors for PDAC. Notably, multivariate analysis revealed that *PLAU* protein upregulation in association with ITGA3, and PPP1R14B expression, tumour stage, and smoking history could predict poor overall survival in PDAC. Overexpression of ITGA3 was confirmed in PDAC clinical specimens and associated with poor prognosis (121). Pan-cancer analysis revealed that increased PPP1R14B expression correlated with poor prognosis and increased immune infiltration levels in myeloid-derived suppressor cells (MDSCs), and PPP1R14B could be used as a prognostic biomarker for pan-cancer (122).

The systematic approach used in this study, based on integrated proteotranscriptomics data, supports a major role for the *PLAU* gene and its corresponding protein (uPA) in driving an aggressive metastatic phenotype of PDAC associated with an immunosuppressed TME. The challenge in using this knowledge to develop *PLAU*-targeted treatment is the well-known heterogeneity of this disease. Therefore, accurate patient stratification is essential to ensure optimal outcomes of targeted therapies. To this end, this study also sought to identify whether specific subtypes of PDAC were associated with *PLAU* upregulation. As noted earlier, the commonest classification of PDAC is based on the morphological features of the tumour, with patients being classified as having classical or basal-like subtypes of PDAC (123). Interestingly, this study found a strong correlation between PLAU upregulation and basal type of PDAC while negatively correlated with classical type gene signatures. Pathway analysis further revealed that *PLAU* upregulation was directly associated with vital oncogenic pathways (WNT, WNT

beta-Catenin (93, 124, 125) and EMT (TGF beta (126) pathways as well as with hypoxia and ECM-rich stroma, all characteristic of basal PDAC (127–129). Finally, the acquisition of all the malignant phenotypes in the high PLAU group supports the basal type PDAC association with *PLAU*. The association of high *PLAU* with the basal PDAC subtype was also validated at the protein level using the CPTAC-PDAC cohort, as was the correlation of the basal subtype with poor survival (Figures 13B-D and SF7).

Importantly, we have validated the concept of a key role for *PLAU*/uPA in cancer progression and its potential as a therapeutic target by performing studies in an orthotopic pancreatic tumour model. Our underlying initial strategy for this study was also to compare a non-chemotherapy targeted approach (uPA inhibitor) with a single agent well-tolerated chemotherapy so as to minimise toxic effects while, at the same time, potentially increasing treatment efficacy. This approach has resulted in very encouraging results where uPA inhibition alone significantly reduced tumour growth to a degree similar to Gemcitabine. Crucially, uPA inhibition was significantly superior to Gemcitabine in reducing metastasis, with U10-treated mice showing no evidence of metastasis. The inhibition of metastasis by uPA inhibition is likely mediated by the decrease in EMT and stemness evident in U10-treated mice. Using uPA knock-out cells Fang et al. has convincingly demonstrated that the knockdown *PLAU* in KYSE-30 cells exhibited significantly reduced tumour growth and weight than the control (normal uPA expression) group, while the *PLAU* overexpression group exhibited increased tumour growth and weight compared with the control group (27). *In vitro* studies using pancreatic cancer cell lines have shown that the knockdown of uPA reduces cancer cell migration, invasion and viability (130).Multiple *in vivo* studies have shown that inhibiting uPA with antibodies, uPA-directed prodrugs or radioisotopes and small molecule inhibitors alone or in combination with other drugs can block cancer growth, invasion and metastasis in prostate and breast cancer (131–135). In addition, uPA inhibitors have also demonstrated very encouraging outcomes in clinical trials for the treatment of different types of solid tumours (136, 137), including using Upamostat (WX-671, Mesupron) in advanced pancreatic cancer patients (138, 139).

This study has yielded novel findings regarding *PLAU* and its role in PDAC tumour progression using comprehensive and integrated transcriptomic/proteomic bioinformatic analyses. Moreover, since upregulation of *PLAU* levels is also frequently observed in a number of malignancies and upregulation of *PLAU* is a prognostic marker not only in pancreatic cancer but also in head and neck, endometrial cancer, renal and lung (42), breast (140) and oesophageal cancer (27). In light of the above, it is highly likely that the approach used in our study for pancreatic cancer could be a promising approach for several other cancers. However, the study does have limitations. All clinical cohorts in

this study (with small sample size) primarily comprised Caucasians or Africans; therefore, caution must be exercised to extrapolate the findings to patients of other ethnicities. The orthotopic xenograft model of pancreatic cancer used in this study involved using a mixture of human cancer cells and human pancreatic stellate cells that provided strong support for our concept that uPA drives pancreatic cancer progression. However, the mice were necessarily immunodeficient, and as such, the model did not lend itself to characterise any immune infiltration into the tumours accurately. The findings derived from our *in silico* and *in vivo* analyses need to be validated experimentally in more depth, a step currently being pursued in our laboratory. In this regard, we are evaluating the effects of inhibiting uPA in a clinically representative orthotopic mouse model (early and advanced) of PDAC in both immune-deficient and immune-competent (syngeneic KPC model, where a mixture of mouse cancer cells and mouse pancreatic stellate cells is implanted into the KPC mouse pancreas) settings with more numbers of mice. The immune cell landscape in this model closely resembles that of human pancreatic cancer with infiltration of myeloid-derived suppressor cells (MDSC), Treg cells and a few CD8+ cytotoxic T cells (141–143). Future work will also combine inhibition with multiagent chemotherapy to further optimise outcomes or to demonstrate that single-agent chemotherapy + targeted therapy may be preferred to current multiagent strategies in selected patients. In search of treatment alternatives, we also hypothesise that in basal-like tumours, since upregulation of the PLAU group has higher hypoxia scores and higher immunosuppressive tumour signatures (PD-L1 and PD-L2) than the anti-tumour immune signature (CD8+ T cells), which may be predictive of immunotherapy (in combination with uPA and plus-minus chemotherapy) in this chemo resistant.

5 Conclusion

For the first time, this study has comprehensively revealed the significance of PLAU in PDAC development, metastasis, and immune suppression and has demonstrated the potential translational importance of inhibiting master regulator PLAU protein in basal type PDAC patients. Thus, it would not be unreasonable to hypothesise that selectively inhibiting PLAU (with and without chemo/immune therapy) in patients with basal PDAC may represent a novel and effective therapeutic approach to improve patient outcomes.

Data availability statement

Publicly available datasets were analyzed in this study. This data can be found here: https://www.ncbi.nlm.nih.gov/gds), Cancer Cell Line Encyclopedia (CCLE, https://depmap.org/portal/ccle/), International Cancer Genome Consortium

(ICGC, https://icgc.org/), the Cancer Genome Atlas (TCGA, http://cancergenome.nih.gov/), the National Cancer Institute's Clinical Proteomic Tumor Analysis Consortium (CPTAC, https://pdc.cancer.gov/pdc/) and the Ontario Institute for Cancer Research (OICR) PDAC cohort' gene expression and clinical data are only available upon through a data access agreement with referenced institute.

Ethics statement

The animal study was reviewed and approved by University of New South Wales Animal Care and Ethics Committee (Approval Number 18/125B) and accomplished under ARRIVE guidelines.

Author contributions

SH. designed experiments, acquired and analysed data, interpreted results, and wrote and revised the manuscript. MU helped analysed data and interpret bioinformatics results. ZX acquired data for *in vivo* experiments; BB synthesized and prepared formulation for *in vivo* study. CP acquired data for *in vitro* experiments. TP helped to interpret the results. AM acquired data for *in vivo* experiments. MM helped to interpret the bioinformatics results. FN and SG acquired OICR-cohort data. RP helped to interpret results and revised manuscript. JW helped to interpret results and revised manuscript. MR helped to interpret results and revised manuscript. DG helped to interpret results, and revised manuscript and MA conceived, designed the study and experiments, interpreted results, and revised manuscript. All authors contributed to the article and approved the submitted version.

Conflict of interest

The authors declare that the research was conducted in the absence of any commercial or financial relationships that could be construed as a potential conflict of interest.

Publisher's note

All claims expressed in this article are solely those of the authors and do not necessarily represent those of their affiliated organizations, or those of the publisher, the editors and the reviewers. Any product that may be evaluated in this article, or claim that may be made by its manufacturer, is not guaranteed or endorsed by the publisher.

Supplementary material

The Supplementary Material for this article can be found online at: https://www.frontiersin.org/articles/10.3389/fimmu.2022.1060957/full#supplementary-material

References

1. Sung H, Ferlay J, Siegel RL, Laversanne M, Soerjomataram I, Jemal A, et al. Global cancer statistics 2020: GLOBOCAN estimates of incidence and mortality worldwide for 36 cancers in 185 countries. *CA: Cancer J Clin* (2021) 71(3):209–49. doi: 10.3322/caac.21660

2. Rahib L, Smith BD, Aizenberg R, Rosenzweig AB, Fleshman JM, Matrisian LM. Projecting cancer incidence and deaths to 2030: The unexpected burden of thyroid, liver, and pancreas cancers in the united states. *Cancer Res* (2014) 74 (11):2913–21. doi: 10.1158/0008-5472.CAN-14-0155

3. Chun JW, Lee SH, Kim JS, Park N, Huh G, Cho IR, et al. Comparison between FOLFIRINOX and gemcitabine plus nab-paclitaxel including sequential treatment for metastatic pancreatic cancer: A propensity score matching approach. *BMC Cancer* (2021) 21(1):537. doi: 10.1186/s12885-021-08277-7

4. Bailey P, Chang DK, Nones K, Johns AL, Patch A-M, Gingras M-C, et al. Genomic analyses identify molecular subtypes of pancreatic cancer. *Nature* (2016) 531(7592):47–52. doi: 10.1038/nature16965

5. Collisson EA, Sadanandam A, Olson P, Gibb WJ, Truitt M, Gu S, et al. Subtypes of pancreatic ductal adenocarcinoma and their differing responses to therapy. *Nat Med* (2011) 17(4):500–3. doi: 10.1038/nm.2344

6. Moffitt RA, Marayati R, Flate EL, Volmar KE, Loeza SGH, Hoadley KA, et al. Virtual microdissection identifies distinct tumor-and stroma-specific subtypes of pancreatic ductal adenocarcinoma. *Nat Genet* (2015) 47(10):1168–78. doi: 10.1038/ng.3398

7. Kumar AA, Buckley BJ, Ranson M. The urokinase plasminogen activation system in pancreatic cancer: Prospective diagnostic and therapeutic targets. *Biomolecules* (2022) 12(2):152. doi: 10.3390/biom12020152

8. Chan-Seng-Yue M, Kim JC, Wilson GW, Ng K, Figueroa EF, O'Kane GM, et al. Transcription phenotypes of pancreatic cancer are driven by genomic events during tumor evolution. *Nat Genet* (2020) 52(2):231–40. doi: 10.1038/s41588-019-0566-9

9. Puleo F, Nicolle R, Blum Y, Cros J, Marisa L, Demetter P, et al. Stratification of pancreatic ductal adenocarcinomas based on tumor and microenvironment features. *Gastroenterology* (2018) 155(6):1999–2013. e3. doi: 10.1053/j.gastro.2018.08.033

10. Kim S, Kang MJ, Lee S, Bae S, Han S, Jang J-Y, et al. Identifying molecular subtypes related to clinicopathologic factors in pancreatic cancer. *Biomed Eng Online* (2014) 13(2):1–11. doi: 10.1186/1475-925X-13-S2-S5

11. Namkung J, Kwon W, Choi Y, Yi SG, Han S, Kang MJ, et al. Molecular subtypes of pancreatic cancer based on miRNA expression profiles have independent prognostic value. *J Gastroenterol Hepatol* (2016) 31(6):1160–7. doi: 10.1111/jgh.13253

12. Janky RS, Binda MM, Allemeersch J, Govaere O, Swinnen JV, Roskams T, et al. Prognostic relevance of molecular subtypes and master regulators in pancreatic ductal adenocarcinoma. *BMC Cancer* (2016) 16(1):1–15. doi: 10.1186/s12885-016-2540-6

13. Birnbaum DJ, Finetti P, Birnbaum D, Mamessier E, Bertucci F. Validation and comparison of the molecular classifications of pancreatic carcinomas. *Mol Cancer* (2017) 16(1):1–7. doi: 10.1186/s12943-017-0739-z

14. Moore MJ, Goldstein D, Hamm J, Figer A, Hecht JR, Gallinger S, et al. Erlotinib plus gemcitabine compared with gemcitabine alone in patients with advanced pancreatic cancer: A phase III trial of the national cancer institute of Canada clinical trials group. *J Clin Oncol* (2007) 25(15):1960–6. doi: 10.1200/JCO.2006.07.9525

15. Royal RE, Levy C, Turner K, Mathur A, Hughes M, Kammula US, et al. Phase 2 trial of single agent ipilimumab (anti-CTLA-4) for locally advanced or metastatic pancreatic adenocarcinoma. *J Immunother (Hagerstown Md: 1997)* (2010) 33(8):828. doi: 10.1097/CJI.0b013e3181eec14c

16. Le DT, Lutz E, Uram JN, Sugar EA, Onners B, Solt S, et al. Evaluation of ipilimumab in combination with allogeneic pancreatic tumor cells transfected with a GM-CSF gene in previously treated pancreatic cancer. *J Immunother (Hagerstown Md: 1997)* (2013) 36(7):382. doi: 10.1097/CJI.0b013e31829fb7a2

17. O'Reilly EM, Oh D-Y, Dhani N, Renouf DJ, Lee MA, Sun W, et al. Durvalumab with or without tremelimumab for patients with metastatic pancreatic ductal adenocarcinoma: A phase 2 randomized clinical trial. *JAMA Oncol* (2019) 5(10):1431–8. doi: 10.1001/jamaoncol.2019.1588

18. Wilson J, Pirola R, Apte M. Stars and stripes in pancreatic cancer: Role of stellate cells and stroma in cancer progression. *Front Physiol* (2014) 5(52). doi: 10.3389/fphys.2014.00052

19. Apte MV, Xu Z, Pothula S, Goldstein D, Pirola RC, Wilson JS. Pancreatic cancer: The microenvironment needs attention too! *Pancreatology* (2015) 15(4 Suppl):S32–8. doi: 10.1016/j.pan.2015.02.013

20. Schnittert J, Bansal R, Prakash J. Targeting pancreatic stellate cells in cancer. *Trends Cancer* (2019) 5(2):128–42. doi: 10.1016/j.trecan.2019.01.001

21. Pothula SP, Xu Z, Goldstein D, Merrett N, Pirola RC, Wilson JS, et al. Targeting the HGF/c-MET pathway: Stromal remodelling in pancreatic cancer. *Oncotarget* (2017) 8(44):76722. doi: 10.18632/oncotarget.20822

22. Bauer TW, Liu W, Fan F, Camp ER, Yang A, Somcio RJ, et al. Targeting of urokinase plasminogen activator receptor in human pancreatic carcinoma cells inhibits c-Met–and insulin-like growth factor-I receptor–mediated migration and invasion and orthotopic tumor growth in mice. *Cancer Res* (2005) 65(17):7775–81. doi: 10.1158/0008-5472.CAN-05-0946

23. Tincknell G, Piper A-K, Aghmesheh M, Becker T, Vine KL, Brungs D, et al. Experimental and clinical evidence supports the use of urokinase plasminogen activation system components as clinically relevant biomarkers in gastroesophageal adenocarcinoma. *Cancers (Basel)* (2021) 13(16):4097. doi: 10.3390/cancers13164097

24. Ranson M, Andronicos NM. Plasminogen binding and cancer: promises and pitfalls. *Front Biosci* (2003) 8:s294–304. doi: 10.2741/1044

25. De Vries T, Van Muijen G, Ruiter D. The plasminogen activation system in tumour invasion and metastasis. *Pathol-Res Prac* (1996) 192(7):718–33. doi: 10.1016/S0344-0338(96)80094-X

26. Chen G, Sun J, Xie M, Yu S, Tang Q, Chen L. PLAU promotes cell proliferation and epithelial-mesenchymal transition in head and neck squamous cell carcinoma. *Front Genet* (2021) 12. doi: 10.3389/fgene.2021.651882

27. Fang L, Che Y, Zhang C, Huang J, Lei Y, Lu Z, et al. PLAU directs conversion of fibroblasts to inflammatory cancer-associated fibroblasts, promoting esophageal squamous cell carcinoma progression *via* uPAR/Akt/NF-κB/IL8 pathway. *Cell Death Discov* (2021) 7(1):1–14. doi: 10.1038/s41420-021-00410-6

28. Bekes EM, Deryugina EI, Kupriyanova TA, Zajac E, Botkjaer KA, Andreasen PA, et al. Activation of pro-uPA is critical for initial escape from the primary tumor and hematogenous dissemination of human carcinoma cells. *Neoplasia* (2011) 13(9):806–21. doi: 10.1593/neo.11704

29. Irigoyen JP, Munoz-Canoves P, Montero L, Koziczak M, Nagamine Y. The plasminogen activator system: biology and regulation. *Cell Mol Life Sciences: CMLS* (1999) 56(1-2):104–32. doi: 10.1007/PL00000615

30. Montuori N, Rossi G, Ragno P. Post-transcriptional regulation of gene expression in the plasminogen activation system. *Biol Chem* (2002) 383(1):47–53. doi: 10.1515/BC.2002.005

31. Nagamine Y, Medcalf RL, Munoz-Canoves P. Transcriptional and posttranscriptional regulation of the plasminogen activator system. *Thromb Haemostasis* (2005) 93(4):661–75. doi: 10.1160/TH04-12-0814

32. Duffy M, Duggan C. The urokinase plasminogen activator system: a rich source of tumour markers for the individualised management of patients with cancer. *Clin Biochem* (2004) 37(7):541–8. doi: 10.1016/j.clinbiochem.2004.05.013

33. Mahmood N, Mihalcioiu C, Rabbani SA. Multifaceted role of the urokinase-type plasminogen activator (uPA) and its receptor (uPAR): Diagnostic, prognostic, and therapeutic applications. *Front Oncol* (2018) 8(24):. doi: 10.3389/fonc.2018.00024

34. Masucci MT, Minopoli M, Di Carluccio G, Motti ML, Carriero MV. Therapeutic strategies targeting urokinase and its receptor in cancer. *Cancers (Basel)* (2022) 14(3):498. doi: 10.3390/cancers14030498

35. Carriero MV, Stoppelli MP. The urokinase-type plasminogen activator and the generation of inhibitors of urokinase activity and signaling. *Curr Pharm Des* (2011) 17(19):1944–61. doi: 10.2174/138161211796718143

36. Blasi F, Carmeliet P. uPAR: a versatile signalling orchestrator. *Nat Rev Mol Cell Biol* (2002) 3(12):932–43. doi: 10.1038/nrm977

37. Jo M, Thomas KS, Marozkina N, Amin TJ, Silva CM, Parsons SJ, et al. Dynamic assembly of the urokinase-type plasminogen activator signaling receptor complex determines the mitogenic activity of urokinase-type plasminogen activator. *J Biol Chem* (2005) 280(17):17449–57. doi: 10.1074/jbc.M413141200

38. Smith HW, Marshall CJ. Regulation of cell signalling by uPAR. *Nat Rev Mol Cell Biol* (2010) 11(1):23–36. doi: 10.1038/nrm2821

39. Andreucci E, Laurenzana A, Peppicelli S, Biagioni A, Margheri F, Ruzzolini J, et al. uPAR controls vasculogenic mimicry ability expressed by drug-resistant melanoma cells. *Oncol Res Featuring Preclinical Clin Cancer Ther* (2021) 28(7-8):7–8. doi: 10.3727/096504021X16273798026651

40. Laurenzana A, Margheri F, Biagioni A, Chillà A, Pimpinelli N, Ruzzolini J, et al. EGFR/uPAR interaction as druggable target to overcome vemurafenib acquired resistance in melanoma cells. *EBioMedicine* (2019) 39:194–206. doi: 10.1016/j.ebiom.2018.12.024

41. Gonias SL, Hu J. Urokinase receptor and resistance to targeted anticancer agents. *Front Pharmacol* (2015) 6:154. doi: 10.3389/fphar.2015.00154

42. Uhlén M, Fagerberg L, Hallström BM, Lindskog C, Oksvold P, Mardinoglu A, et al. Tissue-based map of the human proteome. *Science* (2015) 347(6220):1–9. doi: 10.1126/science.1260419

43. Ma Y, Pu Y, Peng L, Luo X, Xu J, Peng Y, et al. Identification of potential hub genes associated with the pathogenesis and prognosis of pancreatic duct adenocarcinoma using bioinformatics meta–analysis of multi–platform datasets. *Oncol Letters* (2019) 18(6):6741–51. doi: 10.3892/ol.2019.11042

44. Pacini C, Dempster JM, Boyle I, Gonçalves E, Najgebauer H, Karakoc E, et al. Integrated cross-study datasets of genetic dependencies in cancer. *Nat Commun* (2021) 12(1):1661. doi: 10.1038/s41467-021-21898-7

45. Ghandi M, Huang FW, Jané-Valbuena J, Kryukov GV, Lo CC, McDonald ER, et al. Next-generation characterization of the cancer cell line encyclopedia. *Nature* (2019) 569(7757):503–8. doi: 10.1038/s41586-019-1186-3

46. Pei H, Li L, Fridley BL, Jenkins GD, Kalari KR, Lingle W, et al. FKBP51 affects cancer cell response to chemotherapy by negatively regulating akt. *Cancer Cell* (2009) 16(3):259–66. doi: 10.1016/j.ccr.2009.07.016

47. Wennerström AB, Lothe IM, Sandhu V, Kure EH, Myklebost O, Munthe E. Generation and characterisation of novel pancreatic adenocarcinoma xenograft models and corresponding primary cell lines. *PloS One* (2014) 9(8):e103873. doi: 10.1371/journal.pone.0103873

48. Jiang J, Azevedo-Pouly AC, Redis RS, Lee EJ, Gusev Y, Allard D, et al. Globally increased ultraconserved noncoding RNA expression in pancreatic adenocarcinoma. *Oncotarget* (2016) 7(33):53165–77. doi: 10.18632/oncotarget.10242

49. Lin J, Wu YJ, Liang X, Ji M, Ying HM, Wang XY, et al. Network-based integration of mRNA and miRNA profiles reveals new target genes involved in pancreatic cancer. *Mol Carcinog* (2019) 58(2):206–18. doi: 10.1002/mc.22920

50. Gao J, Aksoy BA, Dogrusoz U, Dresdner G, Gross B, Sumer SO, et al. Integrative analysis of complex cancer genomics and clinical profiles using the cBioPortal. *Sci Signaling* (2013) 6(269):pl1. doi: 10.1126/scisignal.2004088

51. Benjamini Y, Hochberg Y. Controlling the false discovery rate: a practical and powerful approach to multiple testing. *J R Stat Society: Ser B (Methodological)* (1995) 57(1):289–300. doi: 10.1111/j.2517-6161.1995.tb02031.x

52. Liberzon A, Subramanian A, Pinchback R, Thorvaldsdóttir H, Tamayo P, Mesirov JP. Molecular signatures database (MSigDB) 3. 0. *Bioinf* (2011) 27(12):1739–40. doi: 10.1093/bioinformatics/btr260

53. Subramanian A, Tamayo P, Mootha VK, Mukherjee S, Ebert BL, Gillette MA, et al. Gene set enrichment analysis: A knowledge-based approach for interpreting genome-wide expression profiles. *Proc Natl Acad Sci United States America* (2005) 102(43):15545–50. doi: 10.1073/pnas.0506580102

54. Szklarczyk D, Gable AL, Lyon D, Junge A, Wyder S, Huerta-Cepas J, et al. STRING v11: protein–protein association networks with increased coverage,

supporting functional discovery in genome-wide experimental datasets. *Nucleic Acids Res* (2019) 47(D1):D607–13. doi: 10.1093/nar/gky1131

55. Shannon P, Markiel A, Ozier O, Baliga NS, Wang JT, Ramage D, et al. Cytoscape: A software environment for integrated models of biomolecular interaction networks. *Genome Res* (2003) 13(11):2498–504. doi: 10.1101/gr.1239303

56. Chin CH, Chen SH, Wu HH, Ho CW, Ko MT, Lin CY. cytoHubba: Identifying hub objects and sub-networks from complex interactome. *BMC Syst Biol* (2014) 8 Suppl 4(Suppl 4):S11. doi: 10.1186/1752-0509-8-S4-S11

57. Cran, R foundation: Therneau T. M. *A Package for Survival Analysis in R.* (2020). Available at: https://CRAN.R-projectorg/package=survival.

58. Yoshihara K, Shahmoradgoli M, Martínez E, Vegesna R, Kim H, Torres-Garcia W, et al. Inferring tumour purity and stromal and immune cell admixture from expression data. *Nat Commun* (2013) 4(1):2612. doi: 10.1038/ncomms3612

59. Bachem MG, Schneider E, Groß H, Weidenbach H, Schmid RM, Menke A, et al. Identification, culture, and characterization of pancreatic stellate cells in rats and humans. *Gastroenterology* (1998) 115(2):421–32. doi: 10.1016/S0016-5085(98)70209-4

60. Apte M, Haber P, Applegate T, Norton I, McCaughan G, Korsten M, et al. Periacinar stellate shaped cells in rat pancreas: identification, isolation, and culture. *Gut* (1998) 43(1):128–33. doi: 10.1136/gut.43.1.128

61. Pothula SP, Xu Z, Goldstein D, Biankin AV, Pirola RC, Wilson JS, et al. Hepatocyte growth factor inhibition: a novel therapeutic approach in pancreatic cancer. *Br J Cancer* (2016) 114(3):269–80. doi: 10.1038/bjc.2015.478

62. Vonlaufen A, Phillips PA, Xu Z, Goldstein D, Pirola RC, Wilson JS, et al. Pancreatic stellate cells and pancreatic cancer cells: an unholy alliance. *Cancer Res* (2008) 68(19):7707–10. doi: 10.1158/0008-5472.CAN-08-1132

63. Xu Z, Pang TCY, Liu AC, Pothula SP, Mekapogu AR, Perera CJ, et al. Targeting the HGF/c-MET pathway in advanced pancreatic cancer: A key element of treatment that limits primary tumour growth and eliminates metastasis. *Br J Cancer* (2020) 122(10):1486–95. doi: 10.1038/s41416-020-0782-1

64. Buckley BJ, Aboelela A, Minaei E, Jiang LX, Xu Z, Ali U, et al. 6-substituted hexamethylene amiloride (HMA) derivatives as potent and selective inhibitors of the human urokinase plasminogen activator for use in cancer. *J Medicinal Chem* (2018) 61(18):8299–320. doi: 10.1021/acs.jmedchem.8b00838

65. Kalimuthu S N, Wilson GW, Grant RC, Seto M, O'Kane G, Vajpeyi R, et al. Morphological classification of pancreatic ductal adenocarcinoma that predicts molecular subtypes and correlates with clinical outcome. *Gut* (2020) 69(2):317–28. doi: 10.1136/gutjnl-2019-318217

66. Pothula SP, Pirola RC, Wilson JS, Apte MV. Pancreatic stellate cells: Aiding and abetting pancreatic cancer progression. *Pancreatology* (2020) 20(3):409–18. doi: 10.1016/j.pan.2020.01.003

67. Vonlaufen A, Joshi S, Qu C, Phillips PA, Xu Z, Parker NR, et al. Pancreatic stellate cells: partners in crime with pancreatic cancer cells. *Cancer Res* (2008) 68(7):2085–93. doi: 10.1158/0008-5472.CAN-07-2477

68. Xu Z, Vonlaufen A, Phillips PA, Fiala-Beer E, Zhang X, Yang L, et al. Role of pancreatic stellate cells in pancreatic cancer metastasis. *Am J Pathology* (2010) 177(5):2585–96. doi: 10.2353/ajpath.2010.090899

69. Mekapogu A, Pothula S, Pirola R, Wilson J, Apte M. Multifunctional role of pancreatic stellate cells in pancreatic cancer. *Ann Pancreat Cancer* (2019) 2(10):1–15. doi: 10.21037/apc.2019.05.02

70. Tian C, Clauser KR, Öhlund D, Rickelt S, Huang Y, Gupta M, et al. Proteomic analyses of ECM during pancreatic ductal adenocarcinoma progression reveal different contributions by tumor and stromal cells. *Proc Natl Acad Sci* (2019) 116(39):19609–18. doi: 10.1073/pnas.1908626116

71. Deutsch EW, Omenn GS, Sun Z, Maes M, Pernemalm M, Palaniappan KK, et al. Advances and utility of the human plasma proteome. *J Proteome Res* (2021) 20(12):5241–63. doi: 10.1021/acs.jproteome.1c00657

72. Froeling FEM, Casolino R, Pea A, Biankin AV, Chang DK. Precision-panc obo. molecular subtyping and precision medicine for pancreatic cancer. *J Clin Med* (2021) 10(1):149. doi: 10.3390/jcm10010149

73. Rashid NU, Peng XL, Jin C, Moffitt RA, Volmar KE, Belt BA, et al. Purity independent subtyping of tumors (PurIST), a clinically robust, single-sample classifier for tumor subtyping in pancreatic cancer. *Clin Cancer Res* (2020) 26(1):82–92. doi: 10.1158/1078-0432.CCR-19-1467

74. Somerville TD, Xu Y, Miyabayashi K, Tiriac H, Cleary CR, Maia-Silva D, et al. TP63-mediated enhancer reprogramming drives the squamous subtype of pancreatic ductal adenocarcinoma. *Cell Rep* (2018) 25(7):1741–55. e7. doi: 10.1016/j.celrep.2018.10.051

75. Ryan DP, Hong TS, Bardeesy N. Pancreatic adenocarcinoma. *N Engl J Med* (2014) 371(11):1039–49. doi: 10.1056/NEJMra1404198

76. Conroy T, Desseigne F, Ychou M, Bouché O, Guimbaud R, Bécouarn Y, et al. FOLFIRINOX versus gemcitabine for metastatic pancreatic cancer. *New Engl J Med* (2011) 364(19):1817–25. doi: 10.1056/NEJMoa1011923

77. Von Hoff DD, Ervin T, Arena FP, Chiorean EG, Infante J, Moore M, et al. Increased survival in pancreatic cancer with nab-paclitaxel plus gemcitabine. *N Engl J Med* (2013) 369(18):1691–703. doi: 10.1056/NEJMoa1304369

78. Conroy T, Hammel P, Hebbar M, Ben Abdelghani M, Wei AC, Raoul J-L, et al. FOLFIRINOX or gemcitabine as adjuvant therapy for pancreatic cancer. *N Engl J Med* (2018) 379(25):2395–406. doi: 10.1056/NEJMoa1809775

79. Nielsen A, Scarlett CJ, Samra JS, Gill A, Li Y, Allen BJ, et al. Significant overexpression of urokinase-type plasminogen activator in pancreatic adenocarcinoma using real-time quantitative reverse transcription polymerase chain reaction. *J Gastroenterol Hepatol* (2005) 20(2):256–63. doi: 10.1111/j.1440-1746.2004.03531.x

80. Cantero D, Friess H, Deflorin J, Zimmermann A, Bründler M, Riesle E, et al. Enhanced expression of urokinase plasminogen activator and its receptor in pancreatic carcinoma. *Br J Cancer* (1997) 75(3):388–95. doi: 10.1038/bjc.1997.63

81. Feilchenfeldt J, Bründler M-A, Soravia C, Tötsch M, Meier CA. Peroxisome proliferator-activated receptors (PPARs) and associated transcription factors in colon cancer: reduced expression of PPARγ-coactivator 1 (PGC-1). *Cancer Letters* (2004) 203(1):25–33. doi: 10.1016/j.canlet.2003.08.024

82. Zhang Y, Ba Y, Liu C, Sun G, Ding L, Gao S, et al. PGC-1α induces apoptosis in human epithelial ovarian cancer cells through a PPARγ-dependent pathway. *Cell Res* (2007) 17(4):363–73. doi: 10.1038/cr.2007.11

83. Uddin MN, Li M, Wang X. Identification of transcriptional signatures of colon tumor stroma by a meta-analysis. *J Oncol* (2019) 2019:8752862. doi: 10.1155/2019/8752862

84. Uhlén M, Fagerberg L, Hallström BM, Lindskog C, Oksvold P, Mardinoglu A, et al. Proteomics. tissue-based map of the human proteome. *Science* (2015) 347(6220):1260419. doi: 10.1126/science.1260419

85. Thayer SP, di Magliano MP, Heiser PW, Nielsen CM, Roberts DJ, Lauwers GY, et al. Hedgehog is an early and late mediator of pancreatic cancer tumorigenesis. *Nature* (2003) 425(6960):851–6. doi: 10.1038/nature02009

86. Li C, Heidt DG, Dalerba P, Burant CF, Zhang L, Adsay V, et al. Identification of pancreatic cancer stem cells. *Cancer Res* (2007) 67(3):1030–7. doi: 10.1158/0008-5472.CAN-06-2030

87. Lee CJ, Dosch J, Simeone DM. Pancreatic cancer stem cells. *J Clin Oncol* (2008) 26(17):2806–12. doi: 10.1200/JCO.2008.16.6702

88. Li W, Cao L, Chen X, Lei J, Ma Q. Resveratrol inhibits hypoxia-driven ROS-induced invasive and migratory ability of pancreatic cancer cells *via* suppression of the hedgehog signaling pathway. *Oncol Rep* (2016) 35(3):1718–26. doi: 10.3892/or.2015.4504

89. Pudełko A, Wisowski G, Olczyk K, Koźma EM. The dual role of the glycosaminoglycan chondroitin-6-sulfate in the development, progression and metastasis of cancer. *FEBS J* (2019) 286(10):1815–37. doi: 10.1111/febs.14748

90. Ricciardelli C, Mayne K, Sykes PJ, Raymond WA, McCaul K, Marshall VR, et al. Elevated stromal chondroitin sulfate glycosaminoglycan predicts progression in early-stage prostate cancer. *Clin Cancer Res* (1997) 3(6):983–92.

91. Huang Y-F, Mizumoto S, Fujita M. Novel insight into glycosaminoglycan biosynthesis based on gene expression profiles. *Front Cell Dev Biol* (2021) 9. doi: 10.3389/fcell.2021.709018

92. Zhan T, Rindtorff N, Boutros M. Wnt signaling in cancer. *Oncogene* (2017) 36(11):1461–73. doi: 10.1038/onc.2016.304

93. Zhang Y, Morris JP IV, Yan W, Schofield HK, Gurney A, Simeone DM, et al. Canonical wnt signaling is required for pancreatic carcinogenesis. *Cancer Res* (2013) 73(15):4909–22. doi: 10.1158/0008-5472.CAN-12-4384

94. Sousa CM, Kimmelman AC. The complex landscape of pancreatic cancer metabolism. *Carcinogenesis* (2014) 35(7):1441–50. doi: 10.1093/carcin/bgu097

95. Yang J, Ren B, Yang G, Wang H, Chen G, You L, et al. The enhancement of glycolysis regulates pancreatic cancer metastasis. *Cell Mol Life Sci* (2020) 77(2):305–21. doi: 10.1007/s00018-019-03278-z

96. Chang C-H, Qiu J, O'Sullivan D, Buck MD, Noguchi T, Curtis JD, et al. Metabolic competition in the tumor microenvironment is a driver of cancer progression. *Cell* (2015) 162(6):1229–41. doi: 10.1016/j.cell.2015.08.016

97. Wellenstein MD, de Visser KE. Cancer-cell-intrinsic mechanisms shaping the tumor immune landscape. *Immunity* (2018) 48(3):399–416. doi: 10.1016/j.immuni.2018.03.004

98. Laurenzana A, Chillà A, Luciani C, Peppicelli S, Biagioni A, Bianchini F, et al. uPA/uPAR system activation drives a glycolytic phenotype in melanoma cells. *Int J Cancer* (2017) 141(6):1190–200. doi: 10.1002/ijc.30817

99. Kierans SJ, Taylor CT. Regulation of glycolysis by the hypoxia-inducible factor (HIF): implications for cellular physiology. *J Physiol* (2021) 599(1):23–37. doi: 10.1113/JP280572

100. Birtolo C, Pham H, Morvaridi S, Chheda C, Go VL, Ptasznik A, et al. Cadherin-11 is a cell surface marker up-regulated in activated pancreatic stellate cells and is involved in pancreatic cancer cell migration. *Am J Pathol* (2017) 187(1):146–55. doi: 10.1016/j.ajpath.2016.09.012

101. Ikenaga N, Ohuchida K, Mizumoto K, Cui L, Kayashima T, Morimatsu K, et al. CD10+ pancreatic stellate cells enhance the progression of pancreatic cancer. *Gastroenterology* (2010) 139(3):1041–51, 51.e1-8. doi: 10.1053/j.gastro.2010.05.084

102. Tang D, Yuan Z, Xue X, Lu Z, Zhang Y, Wang H, et al. High expression of galectin-1 in pancreatic stellate cells plays a role in the development and maintenance of an immunosuppressive microenvironment in pancreatic cancer. *Int J Cancer* (2012) 130(10):2337–48. doi: 10.1002/ijc.26290

103. Qian D, Lu Z, Xu Q, Wu P, Tian L, Zhao L, et al. Galectin-1-driven upregulation of SDF-1 in pancreatic stellate cells promotes pancreatic cancer metastasis. *Cancer Letters* (2017) 397:43–51. doi: 10.1016/j.canlet.2017.03.024

104. Orozco CA, Martinez-Bosch N, Guerrero PE, Vinaixa J, Dalotto-Moreno T, Iglesias M, et al. Targeting galectin-1 inhibits pancreatic cancer progression by modulating tumor-stroma crosstalk. *Proc Natl Acad Sci United States America* (2018) 115(16):E3769–78. doi: 10.1073/pnas.1722434115

105. Yoshida N, Masamune A, Hamada S, Kikuta K, Takikawa T, Motoi F, et al. Kindlin-2 in pancreatic stellate cells promotes the progression of pancreatic cancer. *Cancer Letters* (2017) 390:103–14. doi: 10.1016/j.canlet.2017.01.008

106. Tian L, Lu ZP, Cai BB, Zhao LT, Qian D, Xu QC, et al. Activation of pancreatic stellate cells involves an EMT-like process. *Int J Oncol* (2016) 48(2):783–92. doi: 10.3892/ijo.2015.3282

107. Lee H, Lim C, Lee J, Kim N, Bang S, Lee H, et al. TGF-beta signaling preserves RECK expression in activated pancreatic stellate cells. *J Cell Biochem* (2008) 104(3):1065–74. doi: 10.1002/jcb.21692

108. Horiguchi K, Shirakihara T, Nakano A, Imamura T, Miyazono K, Saitoh M. Role of ras signaling in the induction of snail by transforming growth factor-beta. *J Biol Chem* (2009) 284(1):245–53. doi: 10.1074/jbc.M804777200

109. Kanno A, Satoh K, Masamune A, Hirota M, Kimura K, Umino J, et al. Periostin, secreted from stromal cells, has biphasic effect on cell migration and correlates with the epithelial to mesenchymal transition of human pancreatic cancer cells. *Int J Cancer* (2008) 122(12):2707–18. doi: 10.1002/ijc.23332

110. Ruan K, Bao S, Ouyang G. The multifaceted role of periostin in tumorigenesis. *Cell Mol Life Sci* (2009) 66(14):2219–30. doi: 10.1007/s00018-009-0013-7

111. Kayed H, Jiang X, Keleg S, Jesnowski R, Giese T, Berger MR, et al. Regulation and functional role of the runt-related transcription factor-2 in pancreatic cancer. *Br J Cancer* (2007) 97(8):1106–15. doi: 10.1038/sj.bjc.6603984

112. Mace TA, Bloomston M, Lesinski GB. Pancreatic cancer-associated stellate cells. *OncoImmunology* (2013) 2(7):e24891. doi: 10.4161/onci.24891

113. Nagathihalli NS, Castellanos JA, VanSaun MN, Dai X, Ambrose M, Guo Q, et al. Pancreatic stellate cell secreted IL-6 stimulates STAT3 dependent invasiveness of pancreatic intraepithelial neoplasia and cancer cells. *Oncotarget* (2016) 7 (40):65982–92. doi: 10.18632/oncotarget.11786

114. Tang D, Wang D, Yuan Z, Xue X, Zhang Y, An Y, et al. Persistent activation of pancreatic stellate cells creates a microenvironment favorable for the malignant behavior of pancreatic ductal adenocarcinoma. *Int J Cancer* (2013) 132 (5):993–1003. doi: 10.1002/ijc.27715

115. Sada M, Ohuchida K, Horioka K, Okumura T, Moriyama T, Miyasaka Y, et al. Hypoxic stellate cells of pancreatic cancer stroma regulate extracellular matrix fiber organization and cancer cell motility. *Cancer Letters* (2016) 372(2):210–8. doi: 10.1016/j.canlet.2016.01.016

116. Physico-mechanical aspects of extracellular matrix influences on tumorigenic behaviors. *Semin Cancer Biol* (2010) 20(3):139-45. doi: 10.1016/j.semcancer.2010.04.004

117. Pickup MW, Mouw JK, Weaver VM. The extracellular matrix modulates the hallmarks of cancer. *EMBO Rep* (2014) 15(12):1243–53. doi: 10.15252/embr.201439246

118. Oskarsson T, Acharyya S, Zhang XH, Vanharanta S, Tavazoie SF, Morris PG, et al. Breast cancer cells produce tenascin c as a metastatic niche component to colonize the lungs. *Nat Med* (2011) 17(7):867–74. doi: 10.1038/nm.2379

119. Oskarsson T, Massagué J. Extracellular matrix players in metastatic niches. *EMBO J* (2012) 31(2):254–6. doi: 10.1038/emboj.2011.469

120. Malanchi I, Santamaria-Martínez A, Susanto E, Peng H, Lehr H-A, Delaloye J-F, et al. Interactions between cancer stem cells and their niche govern metastatic colonization. *Nature* (2012) 481(7379):85–9. doi: 10.1038/nature10694

121. Idichi T, Seki N, Kurahara H, Fukuhisa H, Toda H, Shimonosono M, et al. Involvement of anti-tumor miR-124-3p and its targets in the pathogenesis of pancreatic ductal adenocarcinoma: Direct regulation of ITGA3 and ITGB1 by miR-124-3p. *Oncotarget* (2018) 9(48):28849. doi: 10.18632/oncotarget.25599

122. Deng M, Peng L, Li J, Liu X, Xia X, Li G. PPP1R14B is a prognostic and immunological biomarker in pan-cancer. *Front Genet* (2021) 12:763561. doi: 10.3389/fgene.2021.763561

123. O'Kane GM, Grünwald BT, Jang G-H, Masoomian M, Picardo S, Grant RC, et al. GATA6 expression distinguishes classical and basal-like subtypes in advanced pancreatic cancer. *Clin Cancer Res* (2020) 26(18):4901–10. doi: 10.1158/1078-0432.CCR-19-3724

124. Aguilera KY, Dawson DW. WNT ligand dependencies in pancreatic cancer. *Front Cell Dev Biol* (2021) 9. doi: 10.3389/fcell.2021.671022

125. Khramtsov AI, Khramtsova GF, Tretiakova M, Huo D, Olopade OI, Goss KH. Wnt/β-catenin pathway activation is enriched in basal-like breast cancers and predicts poor outcome. *Am J Pathology* (2010) 176(6):2911–20. doi: 10.2353/ajpath.2010.091125

126. Ellenrieder V, Hendler SF, Boeck W, Seufferlein T, Menke A, Ruhland C, et al. Transforming growth factor β1 treatment leads to an epithelial-mesenchymal transdifferentiation of pancreatic cancer cells requiring extracellular signal-regulated kinase 2 activation. *Cancer Res* (2001) 61(10):4222–8.

127. Brunton H, Caligiuri G, Cunningham R, Upstill-Goddard R, Bailey U-M, Garner IM, et al. HNF4A and GATA6 loss reveals therapeutically actionable subtypes in pancreatic cancer. *Cell Rep* (2020) 31(6):107625. doi: 10.1016/j.celrep.2020.107625

128. Connor AA, Denroche RE, Jang GH, Lemire M, Zhang A, Chan-Seng-Yue M, et al. Integration of genomic and transcriptional features in pancreatic cancer reveals increased cell cycle progression in metastases. *Cancer Cell* (2019) 35(2):267–82. e7. doi: 10.1016/j.ccell.2018.12.010

129. Maurer C, Holmstrom SR, He J, Laise P, Su T, Ahmed A, et al. Experimental microdissection enables functional harmonisation of pancreatic cancer subtypes. *Gut* (2019) 68(6):1034–43. doi: 10.1136/gutjnl-2018-317706

130. Wu C-Z, Chu YC, Lai S-W, Hsieh M-S, Yadav VK, Fong I-H, et al. Urokinase plasminogen activator induces epithelial-mesenchymal and metastasis of pancreatic cancer through plasmin/MMP14/TGF-β axis, which is inhibited by 4-acetyl-antroquinonol b treatment. *Phytomedicine* (2022) 100:154062. doi: 10.1016/j.phymed.2022.154062

131. Ossowski L, Russo-Payne H, Wilson EL. Inhibition of urokinase-type plasminogen activator by antibodies: the effect on dissemination of a human tumor in the nude mouse. *Cancer Res* (1991) 51(1):274–81.

132. Towle MJ, Lee A, Maduakor EC, Schwartz CE, Bridges AJ, Littlefield BA. Inhibition of urokinase by 4-substituted benzo [b] thiophene-2-carboxamidines: An important new class of selective synthetic urokinase inhibitor. *Cancer Res* (1993) 53(11):2553–9.

133. Rabbani S, Harakidas P, Davidson DJ, Henkin J, Mazar AP. Prevention of prostate-cancer metastasis *in vivo* by a novel synthetic inhibitor of urokinase-type plasminogen activator (uPA). *Int J Cancer* (1995) 63(6):840–5. doi: 10.1002/ijc.2910630615

134. Xing RH, Mazar A, Henkin J, Rabbani SA. Prevention of breast cancer growth, invasion, and metastasis by antiestrogen tamoxifen alone or in combination with urokinase inhibitor b-428. *Cancer Res* (1997) 57(16):3585–93.

135. Vine K L, Indira Chandran V M, Locke J, Matesic L, Lee J, Skropeta D, et al. Targeting urokinase and the transferrin receptor with novel, anti-mitotic n-alkylisatin cytotoxin conjugates causes selective cancer cell death and reduces tumor growth. *Curr Cancer Drug Targets* (2012) 12(1):64–73. doi: 10.2174/156800912798888983

136. Meyer JE, Brocks C, Graefe H, Mala C, Thäns N, Bürgle M, et al. The oral serine protease inhibitor WX-671–first experience in patients with advanced head and neck carcinoma. *Breast Care* (2008) 3(Suppl 2):20. doi: 10.1159/000151736

137. Goldstein LJ. Experience in phase I trials and an upcoming phase II study with uPA inhibitors in metastatic breast cancer. *Breast Care* (2008) 3(Suppl 2):25. doi: 10.1159/000151733

138. Schmitt M, Harbeck N, Brünner N, Jänicke F, Meisner C, Mühlenweg B, et al. Cancer therapy trials employing level-of-evidence-1 disease forecast cancer biomarkers uPA and its inhibitor PAI-1. *Expert Rev Mol Diagnostics* (2011) 11 (6):617–34. doi: 10.1586/erm.11.47

139. Heinemann V, Ebert MP, Laubender RP, Bevan P, Mala C, Boeck S. Phase II randomised proof-of-concept study of the urokinase inhibitor upamostat (WX-671) in combination with gemcitabine compared with gemcitabine alone in patients with non-resectable, locally advanced pancreatic cancer. *Br J Cancer* (2013) 108(4):766–70. doi: 10.1038/bjc.2013.62

140. Banys-Paluchowski M, Witzel I, Aktas B, Fasching PA, Hartkopf A, Janni W, et al. The prognostic relevance of urokinase-type plasminogen activator (uPA) in the blood of patients with metastatic breast cancer. *Sci Rep* (2019) 9(1):2318. doi: 10.1038/s41598-018-37259-2

141. Mekapogu AR, Xu Z, Pothula SP, Perera C, Pang T, Hosen S, et al eds. *Hepatocyte growth factor/c-met pathway inhibition combined chemotherapy improves tumor immunity and eliminates metastasis in pancreatic cancer*. MARKET ST, PHILADELPHIA: LIPPINCOTT WILLIAMS & WILKINS TWO COMMERCE SQ (2001). PANCREAS; 2021.

142. Yang J, Zhang Q, Wang J, Lou Y, Hong Z, Wei S, et al. Dynamic profiling of immune microenvironment during pancreatic cancer development suggests early intervention and combination strategy of immunotherapy. *EBioMedicine* (2022) 78:103958. doi: 10.1016/j.ebiom.2022.103958

143. Thyagarajan A, Alshehri MSA, Miller KL, Sherwin CM, Travers JB, Sahu RP. Myeloid-derived suppressor cells and pancreatic cancer: Implications in novel therapeutic approaches. *Cancers (Basel)* (2019) 11(11):1627. doi: 10.3390/cancers11111627

Glossary

TCGA	The Cancer Genome Atlas
ICGC	International Cancer Genome Consortium
OICR	Ontario Institute for Cancer Research
CPTAC	Clinical Proteomic Tumor Analysis Consortium
CCLE	Cancer CellLine Encyclopedia
GEPIA	Gene Expression Profiling Interactive Analysis
ACC	adrenocortical carcinoma
BLCA	bladder urothelial carcinoma
BRCA	breast invasive carcinoma
CESC	Cervical squamous cell carcinoma and endocervical adenocarcinoma
CHOL	Cholangiocarcinoma
COAD	colon adenocarcinoma
DLBC	lymphoid neoplasm diffuse large B-cell lymphoma
ESCA	esophageal carcinoma
GBM	glioblastoma multiforme
HNSC	head and neck squamous cell carcinoma
KICH	Kidney chromophobe
KIRC	kidney renal clear cell carcinoma
KIRP	kidney renal papillary cell carcinoma
LAML	acute myeloid leukemia
LGG	brain lower grade glioma
LIHC	Liver hepatocellular carcinoma
LUAD	lung adenocarcinoma
LUSC	lung squamous cell carcinoma
MESO	Mesothelioma
OV	ovarian serous cystadenocarcinoma
PAAD	Pancreatic adenocarcinoma
PCPG	Pheochromocytoma and Paraganglioma
PRAD	prostate adenocarcinoma
READ	rectum adenocarcinoma
SARC	Sarcoma
SKCM	Skin cutaneous melanoma
STAD	stomach adenocarcinoma
TGCT	testicular germ cell tumors
THCA	thyroid carcinoma
THYM	thymoma
UCEC	uterine corpus endometrial carcinoma
UCS	uterine carcinosarcoma
UVM	Uveal Melanoma
HEG	High Expression Group
LEG	Low Expression Group
FDR	false discovery rate
HIF1A	Hypoxia inducible factor 1 subunit alpha
HLAs	human leukocyte antigens
IFN	interferon
MDSCs	myeloid-derived suppressor cells
NK	natural killer

(Continued)

Continued

OS	overall survival
PD-1	Programmed cell death protein 1
PDL1	programmed death-ligand 1
PFI	progression-free interval
SGSs	stromal gene signatures
ssGSEA	single-sample gene-set enrichment analysis
TILs	tumor-infiltrating lymphocytes
OG	Oncogenes
TF	Transcription factors
CK and GF	Cytokines and Growth factors
TCG	Translocating cancer genes
CDM	Cell Differential markers
PK	Protein Kinase
HP	Homeodomain Protein
TS	Tumour Suppressor
EA	Endothelial
STM	Stemness
HYPOX	Hypoxia
CP	Cell Proliferation
ECMD	ECM degradation
ECM	Extracellular Matrix
EMT	Epithelial mesenchymal transition
MTGs	Metastasis-related genes/Metastasis-promoting genes
Ctrl	Control
G	Gemcitabine
	uPA inhibitor (BB2-30F) at 3mg (U3) and 10 mg (U10)
PSCs	Pancreatic stellate cells
PC	Pancreatic cancer
CAhPSCs	Cancer associated human pancreatic stellate cells